DEPARTMENT OF PHYSICS, UNIVERSITY OF JYVÄSKYLÄ
RESEARCH REPORT No. 2/1994

ON THE DYNAMICS OF THE MAGNETOSPHERE BASED ON TIME SERIES ANALYSIS OF GEOMAGNETIC INDICES

BY
JOUNI TAKALO

Academic Dissertation
for the Degree of
Doctor of Philosophy

Jyväskylä, Finland
May 1994

URN:ISBN:978-951-39-9757-1
ISBN 978-951-39-9757-1 (PDF)
ISSN 0075-465X

Jyväskylän yliopisto, 2023

ISBN 951-34-0257-6
ISSN 0075-465X

DEPARTMENT OF PHYSICS, UNIVERSITY OF JYVÄSKYLÄ
RESEARCH REPORT No. 2/1994

ON THE DYNAMICS OF THE MAGNETOSPHERE BASED ON TIME SERIES ANALYSIS OF GEOMAGNETIC INDICES

BY
JOUNI TAKALO

Academic Dissertation
for the Degree of
Doctor of Philosophy

To be presented, by permission of the
Faculty of Mathematics and Natural Sciences
of the University of Jyväskylä,
for public examination in Auditorium S-212 of the
University of Jyväskylä on May 14, 1994,
at 12 o'clock noon

Jyvaskylä, Finland
May 1994

Preface

This work has been carried out at the Department of Physics of the University of Jyväskylä in collaboration with the Department of Geophysics of the Finnish Meteorological Institute during the years 1992-1994. I wish to express my gratitude to my supervisors, Professor Jussi Timonen and Dr. Hannu Koskinen for their valuable advice and encouragement during my work. I have also benefited from discussions with Mr. Raimo Lohikoski and Dr. Johan Silén. Furthermore, I would like to thank the whole personnel of the Department of Physics for providing an inspiring atmosphere.

I am greatful to Associate professor Jorma Kangas from the University of Oulu and Dr. Risto Pirjola from the Finnish Meteorological Institute for refereeing the work.

For financial support I am greatful to the Acadamy of Finland, The Suomen Kulttuurirahasto Foundation, The Magnus Ehrnrooth Foundation, Research Institute for Theoretical Physics of the University of Helsinki, Department of Geophysics of the Finnish Meteorological Institute, and Department of Physics of the University of Jyväskylä.

Finally, I want to thank my wife Marika for her patience and support during my work. I dedicate this thesis to my children Saara and Joonas, who have inspired me throughout this work.

Jyväskylä, April 1994

Jouni Takalo

Abstract

A detailed analysis has been made of 13 periods of 20 days of the AE data. The average correlation dimension is found to be 3.4, and the calculated dimension is found to depend on the magnetospheric activity such that more active periods have smaller dimensions. This apparent correlation dimension does not, however, imply that the magnetospheric system behind the AE data is low-dimensional when studied as an autonomous dynamical system. On the contrary, bicoloured noise is shown to share many properties with the AE data.

It is shown that the AE data have a characteristic autocorrelation time, if properly defined, of approximately 120 minutes (118 ±9 minutes). The structure function (SF) of the AE data shows that the scaling properties of the AE time series change, within error limits, at about the same time scale. For times shorter than 113 (±9) minutes the AE data have a scaling exponent H=0.5, which is similar to that of coloured noise with spectral exponent $\alpha = 2$. After the break the scaling exponent decreases to about 0.15. It is also shown that the scaling properties of the AE data can be directly derived from the autocorrelation function.

It is suggested that the break in the power spectrum of the AE data at a period of approximately 300 minutes is due to the characteristic autocorrelation time of approximately 120 minutes, which is about a half of the critical period in the power spectrum. This is related in turn to the change of the scaling properties of the AE data at about the same characteristic time scale. It seems that the low-frequency part of the power spectrum ($\alpha \approx 1$) mainly arises from the turbulent driving by the solar wind which has a similar power spectrum, whereas the high-frequency part ($\alpha \approx 2$) is more intrinsic to the magnetosphere.

Conventionally the SF has been used to study the affinity of time series. One can easily distinguish a smooth, differentiable time series, for which $H \approx 1$ at small values of λ, from a nondifferentiable fractal curve, for which $0<H<1$. It is shown that the SF can be used in time series analysis also in the case when the time series is not affine, but there appears different scaling behaviour for different time scales. It is further shown that, in addition to the scaling properties, this method can also reveal (quasi)periodic features of the analysed data. The advantage of the method is that it conveniently visualises the periods of the analysed time series.

List of publications

This thesis is a review of the following publications:

I Takalo, J., J. Timonen, and H. Koskinen, Correlation dimension and affinity of AE data and bicolored noise, Geophys. Res. Lett., 20, 1527, 1993.

https://doi.org/10.1029/93GL01596

II Takalo, J., J. Timonen, and H. Koskinen, Dynamics of the magnetosphere as determined from AE and AL data, In Chang T., editor, Physics of Space Plasmas, SPI Conference Proceedings and Reprint series, Number 13, Cambridge, MA, Scientific Publishers, in press, 1994.

III Takalo, J., J. Timonen, and H. Koskinen, Properties of AE data and bicolored noise, J. Geophys. Res., in press, 1994.

https://doi.org/10.1029/94JA00516

IV Takalo, J., and J. Timonen, Characteristic time scale of auroral electrojet data, Geophys. Res. Lett., 21, Number 7, 1994.

https://doi.org/10.1029/94GL00184

V Takalo J., R. Lohikoski, and J. Timonen, Structure function as a tool in AE and Dst time series analysis, submitted to Geophys. Res. Lett., 1994.

https://doi.org/10.1029/95GL00053

The author has mainly written all the papers. The introductory part of the thesis also contains new results which have not been published before, especially the Sections 2.4, 2.5 and 4.4, and some material in Sections 1.2, 2.3, 3.6 and 4.1.

Table of contents

1. Introduction....1
1.1. Structure of the magnetosphere....1
1.2. Dynamics of the magnetosphere....1
1.3. Strange attractor....6
1.4. State space reconstruction....6
1.5. Coloured noise....8

2. Correlation dimension....9
2.1. General....9
2.2. AE data....10
2.3. Coloured noise....11
2.4. Differenced data....12
2.5. Surrogate data....15

3. Structure function....17
3.1. General....17
3.2. Fractal (coloured) noise....17
3.3. AE and AL data....18
3.4. Strange attractor....19
3.5. Dst data....19
3.6. Connections between ACF, SF and the power spectrum....20

4. Other methods....25
4.1. Autocorrelation function....25
4.2. Recurrence plot....27
4.3. A test for determinism in time series....28
4.4. Phase-angle distribution....30

5. Conclusions....33

References....35

1. Introduction

1.1. Structure of the magnetosphere

The magnetosphere is a region around the earth where physical processes are dominated by the geomagnetic field. The basic magnetic field of the earth is nearly a dipole field born inside the earth, but different currents in the magnetosphere deform the geomagnetic field considerably. From outside the field is bounded by the interplanetary magnetic field (IMF) carried by the solar wind whose pressure gives the magnetosphere a "comet-like" form. On the dayside the distance to the border of the magnetosphere, which is called the magnetopause, is about ten earth radii (8-13 R_E), but on the nightside the magnetosphere (magnetospheric tail) extends to a distance of hundreds of R_E.

As mentioned above, there are many current systems in the magnetosphere. On the surface of the earth the magnetic field is almost totally due to sources at the earth's core, but up in the magnetosphere the effect of the magnetospheric currents is of the same size and may occasionally dominate the geomagnetic field. The magnetopause current flows at the border of the magnetosphere mainly from dawn to dusk, and is produced by the solar protons and electrons that try to penetrate into the magnetosphere. Another current system flows through the magnetotail and is called the neutral sheet. It also flows from dawn to dusk and closes in the northern and southern surfaces of the cylindrically shaped magnetotail. The ring current consists of protons and electrons which drift in opposite directions above the equator creating a large scale current system. During a moderate geomagnetic activity the value of the ring current may be millions of amperes, which means a huge amount of energy. In addition the particles move in the north-south direction and are connected to the polar regions, dissipating the stored energy during auroral substorms. The fourth important current system is formed by the auroral electrojets which flow in the ionosphere at the auroral zones. The auroral electrojets are coupled to the magnetosphere via field-aligned currents (see Figure 1).

The configuration of the magnetic field in the magnetosphere depends on the orientation of the IMF. The IMF is predominantly in the ecliptic plane, but also has a significant component in the direction perpendicular to that plane. If this component is directed to the north (northward IMF), the topology of the magnetosphere is closed. When the perpendicular component of the IMF is southward, the magnetosphere becomes open such that the geomagnetic field lines are connected with those of the IMF. In this case solar wind particles can directly enter the magnetosphere [see as general reviews Egeland et al., 1973; Akasofu, 1977; Parks, 1991].

1.2. Dynamics of the magnetosphere

During the last two decades or so it has been known that even very simple nonlinear systems may exhibit very complex behaviour under changing of decisive parameters. Although it may seem that there exists no order in the system, it is not random but may be deterministically chaotic. This means that the system is sensitive to the initial state, and predicting the evolution of the system for long times is impossible. However, this kind of chaotic dynamics may be bounded, and the trajectories of the system are restricted in the state space.

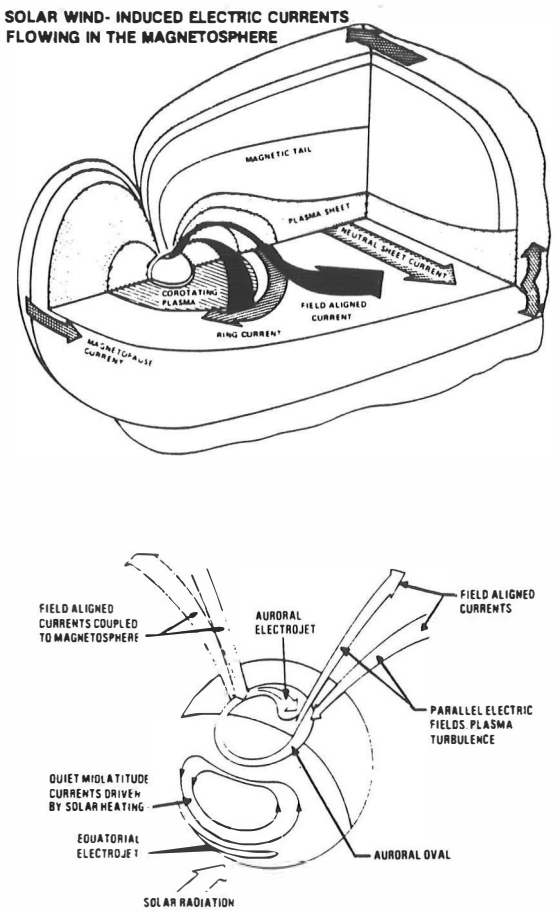

Figure 1. A schematic diagram of the most important current systems of the magnetosphere (upper figure) and ionosphere (lower figure), including field aligned currents that couple magnetosphere to ionosphere (from Parks, [1991]).

Stochastic processes exhibit a large (in some cases infinite) number degrees of freedom, but a complex nonlinear system which contains an attractor can be described by much fewer variables than the original system. These independent variables correspond to the degrees of freedom of the system. When it has become evident that nonlinear systems in nature can be chaotic, new techniques have been brought in for analysing the observed behaviour of dissipative dynamical systems.

One such system, interconnected by electrodynamical forces, is the magnetosphere of the earth. The solar wind carries plasma and energy through the solar system. When the solar wind meets the magnetosphere of the earth, there appears a complex dynamical interaction between them. The magnetosphere is a kind of energy-flow system which, when connected to the interplanetary magnetic field, stores energy, and then, after becoming unstable, releases it to the ionosphere during magnetospheric substorms.

Besides the energy dissipation in the magnetosphere-ionosphere interaction, energy is also released back to the solar wind from the magnetospheric tail via plasmoid formation and disconnection. It has been suggested that this energy release from the tail resembles dripping of a leaky faucet [Hones, 1979] shown in Figure 2. On the other hand, dripping faucet is a classical model of a chaotic system [Shaw, 1984; Martien et al., 1985; Wu and Schelly, 1989]. The flow rate of a dripping faucet is first periodic but becomes for higher flow rates, through period-doublings, chaotic. It is therefore possible that the magnetosphere may globally behave like a chaotic system, at least for a range of energy transfer rates from the solar wind.

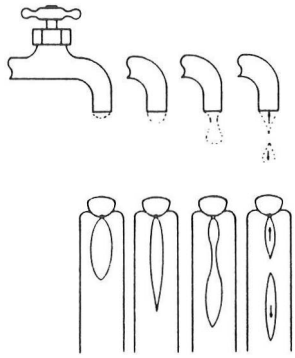

Figure 2. The leaky faucet analogy of the plasmoid formation and release in the magnetospheric tail (from Hones, [1979]).

This possibility is supported by the linear prediction filter analysis [Iyemori et al., 1979; Bargatze et al., 1985]. In this method the relationship between the input time series I(t) and the output time series O(t) is calculated from the equation

$$O(t) = \int_0^\infty H(\tau)\, I(t-\tau)\, d\tau \,, \qquad (1)$$

where $H(\tau)$ is a linear filter (or the impulse response). In Figure 3 we show the impulse response of the magnetosphere using the solar wind VB_s, where V is the solar wind speed and B_s the southward component of the IMF, as the input data, and the magnetospheric AL index (defined later) as the output data [Bargatze et al., 1985]. The filters are arranged from bottom to top in the order of increasing geomagnetic activity. It is evident from this figure that there are clearly two different responses, one at about 20 minutes and another after about an hour. The first peak at 20 minutes is supposed to arise from the direct component of the solar wind while the second peak could arise from the loading-unloading component due to release of stored energy from the magnetospheric tail. A difference between the peaks is that the 20-minute peak is seen throughout the filters while the 1-hour peak first increases in intensity up to the filter of moderate activity and then diappears. This behaviour could be due to the transition of the system from a periodic state to chaotic dynamics. In fact Baker et al. [1990] have introduced an analogue model based on this idea, and Klimas et al. [1992] have introduced a Faraday loop model which is similar to the mechanical dripping faucet analogue but expressed in plasma physical terms.

Several analyses of auroral electrojet indices show that the magnetospheric disturbance data have a low correlation dimension [Vassiliadis et al., 1990; Shan et al., 1991a and 1991b; Roberts et al., 1991; Roberts, 1991; Vörös, 1991; Pavlos et al., 1992; Sharma et al., 1993a; Takalo et al., 1993 and 1994a] which is defined in Chapter 2 below. This result suggests that there may exist an intrinsic strange attractor which governs the dynamics of the magnetosphere. The values of the correlation dimension reported by these authors vary from 2.2 to about 4. On the other hand it has been shown [Prichard and Price, 1992; Takalo et al., 1993] that the modified correlation sum suggested by Theiler [1986] does not lead to saturation of the slopes of the correlation sums.

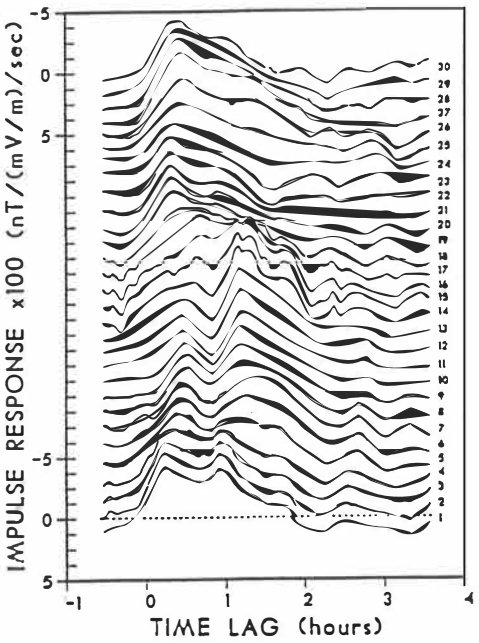

Figure 3. Linear prediction filters of the response of the magnetosphere. The filters are arranged in the ascending order according to their activity level (from Bargatze et al., [1985]).

We have studied the dynamics of the magnetosphere by analysing magnetospheric AE, AL, and Dst indices. The auroral electrojet (AE) index was originally introduced to describe the global activity of the auroral zone electric currents [Davis and Sugiura, 1966]. The AE index is derived from the variations in the horizontal component of the geomagnetic field on the earth's surface. These variations are measured at 12 stations which are almost evenly located near the auroral zone around the northern hemisphere of the earth. All stations determine first the base line value of each month by averaging over the magnetic activity of the five most quiet days of that month. This base line value is then subtracted from every value recorded during that month. From the recordings of all stations the greatest and smallest values are then chosen at intervals of one minute. These values form two indices, the AU and AL index. From

these the AL index describes the lower envelope of the variations and the AU index the upper envelope of the variations. AL and AU indices are also measures for the strongest westward and eastward intensities of the auroral electrojet, respectively. In the auroral ionosphere there may also appear zonal currents which give their contribution to the indices. For this reason it is customary to define the index AE=AU-AL that is independent of the zonal currents. The AE index represents the overall intensity of the auroral electrojets. The power spectra of AE and AL data are known to have a power-law form, $f^{-\alpha}$, such that the spectral exponent changes at a frequency of about 1/(5 hr) [Tsurutani et al., 1990; Takalo et al., 1993]. The spectral exponent is $\alpha \approx 1$ for low frequencies, and $\alpha \approx 2$ for high frequencies. Figure 4 shows the power spectrum of the AE data of 1978-85. The break point where the spectral exponent changes, as calculated from this spectrum, is at 310 minutes with a standard deviation of about 30 minutes. The error lines are shown in figure by dotted lines. The solid lines show linear fits which have been used to evaluate the break points. The standard deviation of the break point has been determined from the standard deviations of the fitting parameters by the law of error propagation. It should be noted that the evaluated break point seems to depend on the used fitting range. However, our result here is compatible with our earlier result 286 ±42 min [Takalo and Timonen, 1994], calculated as an average of one year periods, and also with the results of Tsurutani et al. [1990] who have reported values between 4.7 and 5.5 hours.

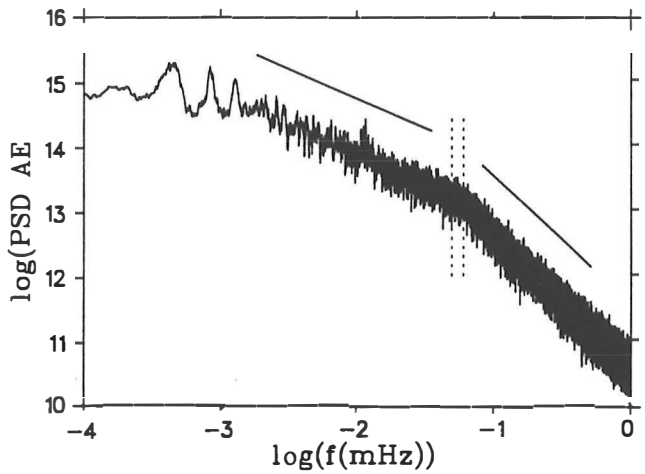

Figure 4. A power spectrum of the AE time series, as calculated from the data of 1978-85. Note the break, marked by vertical dotted lines, in the slope of the spectrum at about $5.6*10^{-2}$ mHz (5-hour period).

The Dst index is recorded at four stations at low latitudes and is assumed to mainly describe the equatorial ring current. The fluctuations in the ring current intensity are not so rapid as in the auroral electrojets, and that is why an equally dense network of stations is not needed for the registration of the Dst data. The baseline and the secular variations are also in this case first subtracted from the data. The Dst index is then averaged over the values of the stations to give D(t), and normalized to the dipole equator by defining

$$Dst(t) = D(t)/\cos\varphi \qquad (2)$$

where φ is the mean dipole latitude of the stations. The resolution of the Dst index is 1 hour.

1.3. Strange attractor

As time evolves a dissipative dynamical system approaches a state which is called an attractor of the system. This can be, e.g. a fixed point, as for a damped pendulum, or a limit periodic cycle, as for a driven and damped oscillator, but may, under certain conditions, be also a much more complex object [Eckmann and Ruelle, 1985]. Let us consider an infinitely small (hyper)ball in an m-dimensional state space. During time evolution, this ball is distorted and becomes an ellipsoid. Denote the principal axes of this ellipsoid by $\varepsilon_i(t)$, (i=1,...,m) [Grassberger and Procaccia, 1983]. The Lyapunov exponents λ_i are then defined by

$$\varepsilon_i(t) \approx \varepsilon_i(0)\, e^{\lambda_i t} \quad . \qquad (3)$$

For a dissipative system the volume of the ellipsoid is of course contracting, and the sum of the Lyapunov exponents is negative. If, however, at least one of these exponents is positive, the motion diverges exponentially in one direction of the state space. In order the motion to be bounded, there has to be contraction in other directions, and the motion is divergent only at small distances. This kind of exponential divergence leads to a sensitive dependence of the motion on the initial conditions. In this case the motion is said to be chaotic, and the resulting attractor is strange. A property of strange attractors is that the cross-section of an attractor with a transverse (hyper)plane in the state space (Poincare section) is fractal. If the points in an m-dimensional state space are evenly distributed in all directions, the number of points within a sphere of radius r is proportional to r^m. In contrast with this, if the distribution of points is fractal, the corresponding number of points is proportinal to r^ν, where $\nu < m$ is noninteger and is called the fractal dimension. This property of a strange attractor results from its structure which is created by successive stretching and folding processes.

1.4. State space reconstruction

When studying complex dynamical systems we quite often encounter a situation where we only know the time evolution of one characteristic quantity of the system. In such cases the time-delay embedding is a good method to construct an artificial state space [Packard et al., 1980, Takens, 1981]. Consider the time series of one variable X(t). Construct m-dimensional vectors

$$\vec{x_i} = \Big(x(t_i),\ x(t_i+\tau),\ \ldots,\ x(t_i+(m-1)\tau)\Big) \ , \qquad (4)$$

where i=1,..,N and τ is an appropriate time lag. These state vectors then form points of the constructed trajectory in the state space. The question is how should we choose the two parameters, the embedding dimension m and the time lag τ.

Sauer et al. [1991] have shown that, if D is the fractal dimension of a strange attractor, there should be at least m dimensions in the state space, where m is the smallest integer greater than 2D. It has also been shown [Sauer et al., 1991; Ding et al. 1993a and 1993b] that the smallest

integer m greater than D should be enough if only the correlation dimension (to be defined in Chapter 2) of the attractor is determined by the embedding method. The delay coordinate map with m>D is, however, not a one-to-one map of the original state space. That is why m>2D is needed, if we are going to extract dynamical information, and predict e.g. the future behaviour of trajectories. To find a large enough m is not a problem because we can increase the embedding dimension until we get satisfying results. However, using an embedding dimension which is unnecessarily large is time consuming.

A bigger problem is to find a good time lag τ. If too small a lag is used, the successive coordinates are almost the same. In this case the reconstructed trajectory stays very close to the straight line which is the diagonal of the state space. This is clearly seen in Figure 5a for the time series of the Lorenz attractor [Lorenz, 1963]. If the time lag is too big, the coordinates are independent and the trajectory is distorted (Figure 5c). There has been a number of studies on the estimation of the time lag by using different characteristic functions.

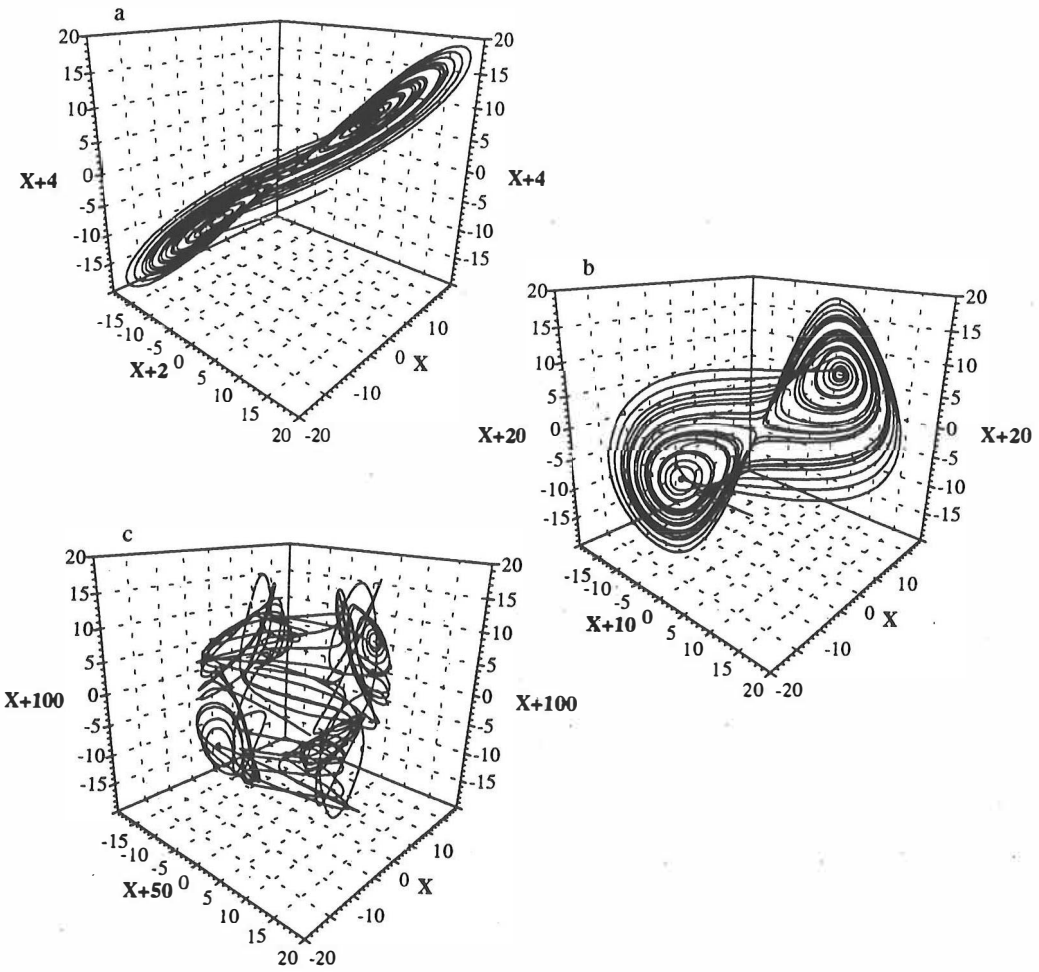

Figure 5. Plots of the Lorenz attractor as calculated from the x-component by the embedding method using time lags of (a) 2 time steps, (b) 10 time steps, and (c) 50 time steps.

purpose the first minimum of the logarithm of the generalized correlation function. Buzug and Pfister [1992] introduced a "fill-factor method" for calculating the optimal time lag.

The most popular method has been to determine the time lag from the autocorrelation function of the studied data. The normalized autocorrelation function (ACF) of time series AE(t) can be expressed in the form [Takalo and Timonen, 1994]

$$AC(\tau_a) = \lim_{T\to\infty} \left\{ \int_0^T dt\, \delta AE(t)\, \delta AE(t+\tau_a) \;\Big/\; \int_0^T dt\, \delta AE^2(t) \right\} \approx (N\sigma^2)^{-1} \sum_{t=1}^{N} \delta AE(t)\, \delta AE(t+\tau_a) \quad (5)$$

where $\delta AE(t) = AE(t) - \langle AE(t) \rangle$ with $\langle AE(t) \rangle$ the average of AE(t), and σ^2 is the variance calculated from N points of the data. Traditionally the autocorrelation time (or decorrelation time) has been defined to be the time when the function decreases to the half (or to 1/e) of the initial value. Sometimes the first minimum or the first zero of the ACF has also been used as a characteristic time scale during which the system loses its memory. However, one of these values is probably a good estimate for the time lag used in the embedding reconstruction as seen in the Figure 5b for the Lorenz attractor with lag 10 time steps.

1.5. Coloured noise

In Section 1.2 we saw that the power spectra of the magnetospheric indices have a power-law form. This fact has been the motivation for us to study a simple class of random noise, the so-called coloured noise. Coloured noise has also a power spectrum of the same form, $f^{-\alpha}$, with $\alpha \geq 1$ ($\alpha \approx 0$ for white noise).

We have generated coloured noise X(j) defined by the expression [Osborne and Provenzale, 1989; Higuchi, 1990; Greis and Greenside, 1991; Takalo et al. 1993 and 1994a]

$$X(j) = \sum_{k=1}^{N/2} \left(P(k) \frac{2\pi}{N} \right)^{1/2} \cos\left(2\pi jk/N - \varphi_k \right) , \quad (6)$$

where j=1,2,...,N is a discrete time index. Randomness comes from the randomized phases φ_k which are defined in the range $[0, 2\pi]$, and

$$P(k) = Qk^{-\alpha}. \quad (7)$$

In order to get noise with a power-spectrum which is similar to that of AE (and AL) data, we have generated coloured noise with two components, and call it bicoloured noise. We have chosen the power spectrum of this bicoloured such that it has $\alpha_L = 1$ for low frequencies, $k < k_c$, and $\alpha_H = 2$ for $k > k_c$. The critical value k_c will be chosen such that it relates to the frequency at which there is a break in the power spectrum of the AE time series. We require further that the power spectrum is continuous which means that [Higuchi, 1990; Takalo et al., 1993]

$$Q_L\, k_c^{-\alpha_L} = Q_H\, k_c^{-\alpha_H} . \quad (8)$$

2. Correlation dimension

2.1. General

To study the distribution of points in the state space we have applied the method by Grassberger and Procaccia (GP)[1983]. For the constructed embedding vectors we calculate the GP correlation sums

$$C_m(r) = \frac{1}{N^2-N} \sum_{i \neq j}^{N} \theta\left(r - \left|\vec{x}_i - \vec{x}_j\right|\right) , \tag{9}$$

where $\theta(x)$ is the Heaviside step function (= 0 for negative and =1 for positive arguments) and $|.|$ means the usual Euclidean distance, although other norms may also be used. If the number of points, N, is large enough, the correlation integral obeys, for small values of r, a power-law,

$$C_m(r) \sim r^{\nu} \quad . \tag{10}$$

Here the exponent ν is called the correlation dimension (one kind of fractal dimension) and it can be determined from the expression

$$\nu = \lim_{r \to 0} \frac{\log(C_m(r))}{\log(r)} \quad . \tag{11}$$

In this work we calculate the slopes d log $(C_m(r))$ / d log (r) between two adjacent r-values and then consider this slope as a function of log(r). If in some scaling region these slopes seem to saturate at a definite value, the correlation dimension ν is defined as the average of the slopes in this scaling region. If ν is noninteger, we assume that it indicates fractal distribution of points in the state space. It also indicates that the next integer greater than the correlation dimension may be the number of independent variables in the original system.

Use of a modified correlation sum [Theiler,1986] has been suggested to prevent spurious dimension estimates caused by strong autocorrelation of the data. The modified correlation sum (correlation integral) is defined by

$$C_2(r) = \frac{2}{(N-W)(N-W+1)} \sum_{j=W}^{N} \sum_{i=1}^{N-j} \theta\left(r - \left|\vec{x}_{i+j} - \vec{x}_i\right|\right) , \tag{12}$$

where W is the number of nearest vectors which are omitted in the sum. The modified correlation sum should not affect the correlation dimension of a strange attractor if there is a long enough time series, because its trajectory returns over and over again close to the starting point. On the other hand, in the case of fractal noise, loosing the points that are close in time is decisive because, as we shall show later, a vast amount of the nearby points inside a given radius in the state space consists of points that are also close in time.

2.2. AE data

In order to find the correlation dimension of the AE data we have studied 13 periods with different levels of geomagnetic activity from the years 1979-85. These periods consist of 28800 points (20 days) of 1-minute AE data. In Figure 6a we show the slopes of the correlation sums for the period beginning on February 1, 1981. The average of the AE index is 177 nT for this period, and the time lag used in the calculation is 100 minutes. The saturation is very good and we find 3.5 for the correlation dimension. In Figure 6b we show the slopes for the period beginning on January 1, 1983. The behaviour of the slopes in this case is more typical of the AE data than the one shown in Figure 6a. The slopes in Figure 6b seem to saturate despite of typical fluctuations, and at greater values of r there are also characteristic "hills" in the plots. The mean activity level of this time series is 217 nT, so the period is moderately disturbed. The average of the slopes with a time lag of 50 minutes is 3.4 in the proper scaling region. Altogether we find that the evaluated correlation dimensions for 13 analysed periods of 20 days vary between 2.9 and 4.2 [Takalo et al., 1994a] The average of all these correlation dimensions is 3.4.

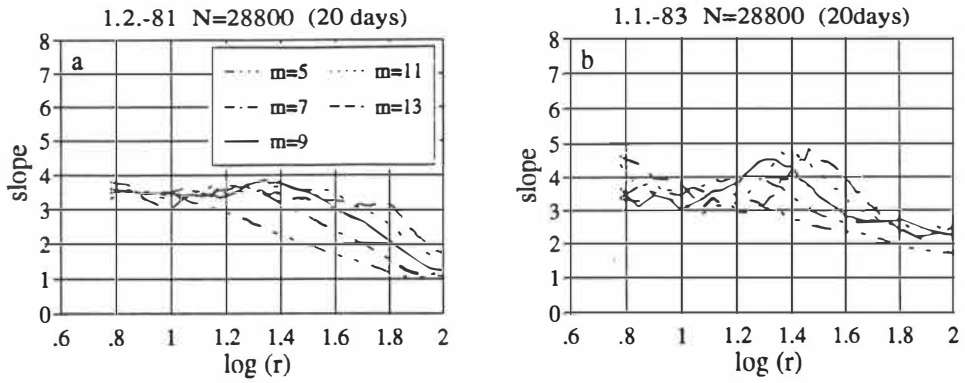

Figure 6. Plots of the slopes of the GP correlation sum for 20-day periods (28800 points) of the AE data beginning on (a) February 1, 1981, and (b) January 1, 1983 (Figure 6a from Takalo et al, [1993], Figure 6b from Takalo et al, [1994a]).

One result from the correlation dimension analysis is that the measured correlation dimension seems to depend on the magnetospheric activity such that more active periods have smaller dimensions. The regression line which is also shown in Figure 7 has a correlation coefficient of r = - 0.77. Here the average activity is determined as the mean value of the AE indices, but we have also determined the activities from the integral occurrence percentages [Bargatze et al., 1985]. This method gives somewhat smaller activities than the mean, but the relationship with the correlation dimension is almost the same. One must admit, however, that 13 points may not give a statistically significant result. It is possible that the decrease in the apparent dimension with increasing activity arises because more disturbed periods may be more nonstationary. This would mean that there is a deeper dip in the scaling region of the slopes, in which case the apparent correlation dimension is correspondingly smaller.

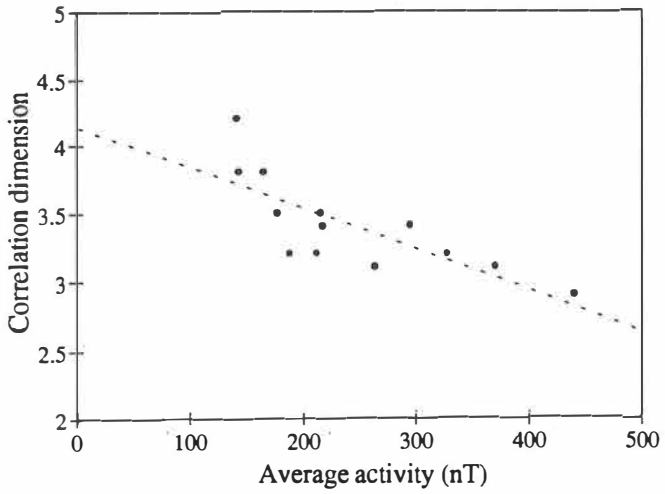

Figure 7. Correlation dimension as a function of average activity for the 13 analysed periods of the AE data (from Takalo et al., [1994a]).

2.3. Coloured noise

The low correlation dimension does not necessarily mean that the system behind the time series exhibits a strange attractor. In fact, coloured noise also leads to a low finite value for the correlation dimension [Osborne and Provenzale, 1989]. This correlation dimension means that the trajectories in the state space exhibit fractal behavior along the trajectory (they are fractal curves), while the fractality of a strange attractor associated with a chaotic system is perpendicular to the motion because each trajectory returns at times close to the starting point. However, it should be noted that the requirement of smoothness in the embedding procedure, i.e. the requirement that the time series is at least twice differentiable [Takens, 1981], is not fulfilled for the coloured noise. Furthermore, the apparent correlation dimension D of monocoloured noise is related to the spectral exponent α by $D \approx 2/(\alpha - 1)$ [Osborne and Provenzale, 1989].

In Figure 8 we show the slopes of the GP correlation sums with a lag of 20 time steps for 7200 points of bicoloured noise with critical frequency $f_c = k_c/N = 1/300$. Although coloured noise with $\alpha = 2$ gives a correlation dimension of about 2, and that with $\alpha = 1$ a dimension over 10 [Osborne and Provenzale, 1989], the mixed bicoloured noise saturates somewhere between these two values. At longer distances the plots of the slopes seem to indicate a bigger value for the dimension, but at smaller values of r the slopes decrease because the steeper part of the spectrum ($\alpha = 2$) dominates. However, the saturation value of the apparent correlation dimension is greater than that for monocoloured noise with $\alpha = 2$. In this way we also find the charasteristic "hills" similar to typical cases of the AE data. The saturation value of the correlation dimension seems to depend upon k_c, where the spectral exponent changes [Takalo et al., 1993].

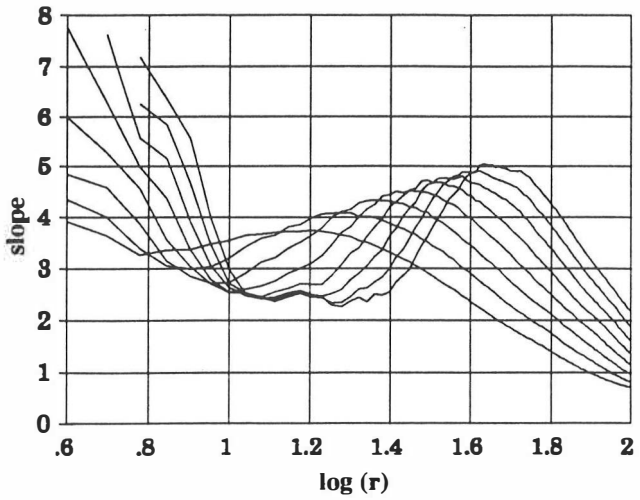

Figure 8. Plots of the slopes for the generated bicoloured noise (N=7200) with a critical frequency of f_c=1/300. The curves are calculated for embedding dimensions m=5,6,...,12 (from bottom to top at log(r)=2) and for a time lag of 20 time steps.

2.4. Differenced data

To prevent the effect of autocorrelation, Theiler [1986] proposed a modified version of the GP correlation sum such that the points inside the autocorrelation time are omitted in the sum. We have used this method and shown that it does not generally lead to saturation of the slopes at a low correlation dimension [Takalo et al., 1993]. However, this method may sometimes be inapplicable because of very long autocorrelation times and the shortness of the available time series.

One way to reduce the effect of autocorrelation in the data is to study the differenced time series (first difference)

$$Y(i) = \Delta X(i) = X(i+1) - X(i) , \tag{13}$$

where X(i) is the original time series [see e.g. Sugihara and May, 1990; Provenzale et al., 1992; Sharma et al., 1993b; Takalo et al., 1994a; Prichard, 1993]. Differentiation could possibly remove the nonstationarity in the mean of the time series [Prichard and Price, 1993b]. Furthermore, the differenced data have a greater density of points in the state space. However, there are also drawbacks in the use of differenced data because differentiation is a kind of high-pass filtering process, and it is known that filtering the data can lead to low-dimensional behaviour [see e.g. Grassberger et al., 1991; Rapp et al., 1993; Vassiliadis and Daglis, 1993].

In the case of a strange attractor, the differenced data should give about the same correlation dimension as the original data [Provenzale et al., 1992]. This is also evident in the Figure 9 where we show the differenced Lorenz attractor (Figure 9a) and the slopes of the GP correlation sum for the differenced Lorenz data (Figure 9b). The correlation dimension is near 2.06 which is the value for the original Lorenz attractor. On the other hand, we could use the differenced time series to distinguish an attractor from coloured noise because the differenced data of coloured noise gives a much bigger value for the correlation dimension than the original data. This can easily be understood because the power spectrum of the differenced

time series of coloured noise is proportional to $f^{-\alpha+2}$, where α is the spectral exponent of the original time series [Higuchi,1990; Takalo et al., 1994a].

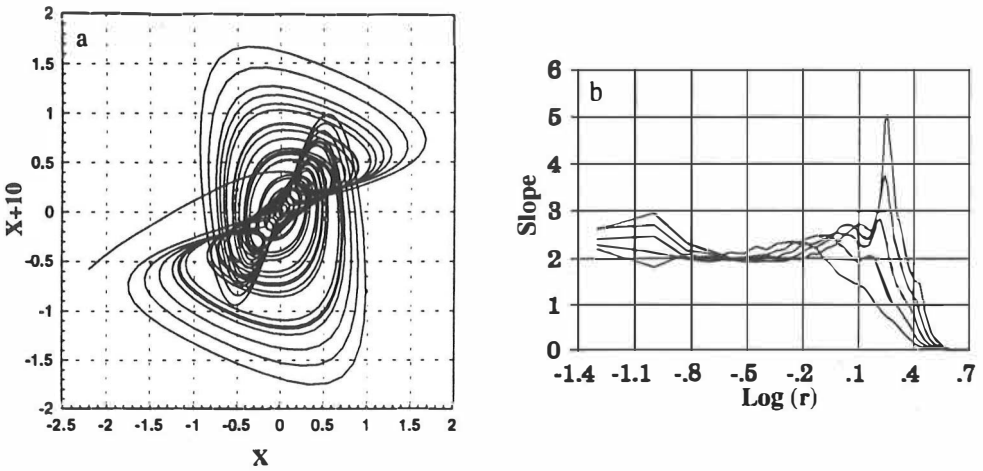

Figure 9. (a) The differenced Lorenz attractor. (b) Plots of the slopes for the differenced Lorenz attractor (N=7200), as calculated for m = 5, 7,..., 13 (from bottom to top at log(r)=0.4), and for a time lag of 10 time steps.

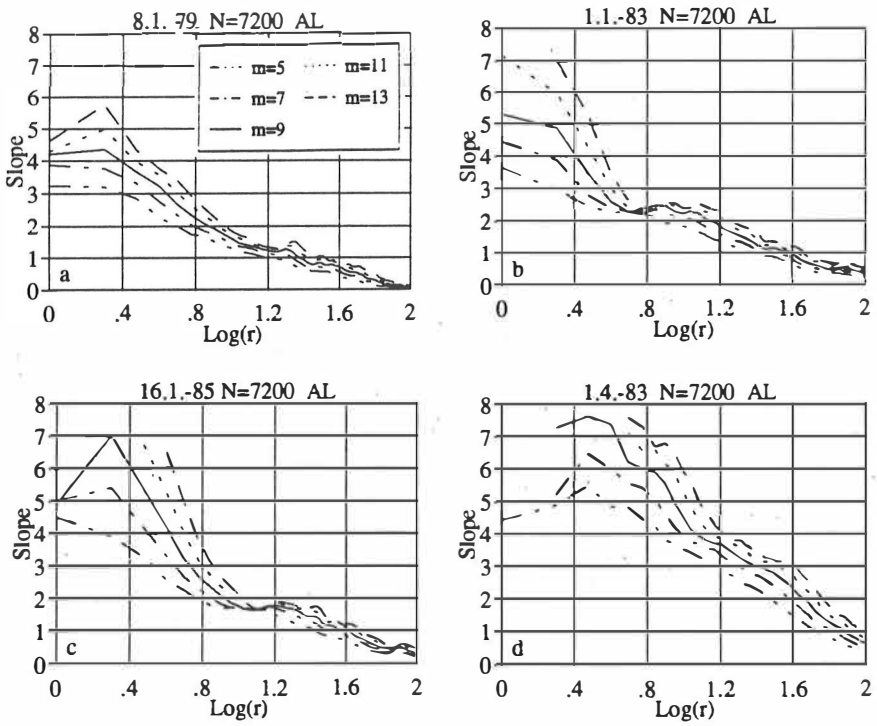

Figure 10. The plots of the slopes for four different time series of the differenced AL data. The curves are calculated with 7200 points using a time lag of 5 min. The figures for different periods are arranged from a to d according to increasing activity level of the data.

In Figure 10 we show the correlation dimension analyses of four different 5-day periods of the differenced AL data. The figures are arranged such that 10a is the result for the most quiet period and 10d that for the most active one. In Figures 10b (beginning on January 1, 1983) and 10c (beginning on January 16, 1985) which show results for moderately active periods, there are quite good plateaus in the plots indicating saturation of the slopes at a correlation dimension of about 2.4 and 1.7, respectively. Is this behaviour due to a strange attractor governing the dynamics of auroral electrojets during moderate active periods of these jets, or is it due to some kind of biasing effect? We must admit that the scaling regions of the plateaus are quite short. It can clearly be seen that, for increasing activity of the period, the plots rise steeper towards smaller distances. However, it seems that the plots do not shoot up in the way they do for totally stochastic data. This kind of behaviour may be caused by the fact that at times the signal, even during the most active periods, stays almost constant. Notice that the correlation dimension of a regular curve is one. This kind of intermittent, "bursty", behaviour of the data has the effect of pushing the slopes downwards [Vassiliadis and Daglis, 1993]. We have also noticed that for some periods of the differenced AL data there seems to be a kind of a plateau in the slopes at a value of one (see Figure 10a). In addition, most of the time the trajectory is confined in a very small volume near the origin of the state space, and, because the values of the data are cut to their integer parts, the state space is very coarse-grained [Grassberger et al., 1991; Prichard, 1993].

To mimic these effects we have generated noise such that the signal consists of random numbers (white noise) inside randomly placed exponential peaks (Figure 11a). In Figure 11b we show the plots of the slopes calculated for 7200 points of such data. The plots seem to rise very slowly towards the smaller distances. This causes an artificial saturation of the slopes at a dimension of about 3, although there are no clear plateaus in the slopes.

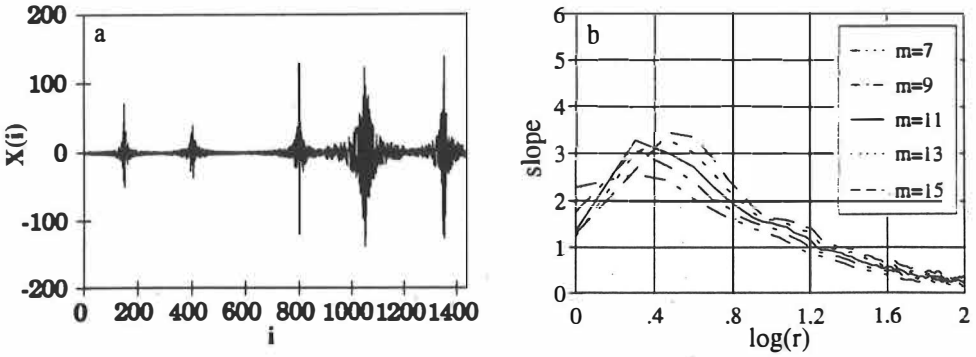

Figure 11. (a) A time series of "white" noise such that the signal consists of random numbers inside randomly placed exponential peaks. (b) The plots of the slopes for the time series of Figure 11a.

2.5. Surrogate data

As a test to distinguish between deterministic chaos and stochastic noise, it has been suggested to use phase randomization of the time series [Roberts, 1991; Provenzale et al., 1992]. If the time series is random, one should not get saturation of the slopes at a low dimension for the phase-randomized data. However, randomizing the phases of AE (or AL) time series changes the data quite a lot. This is because the AE data has very skewed statistics (all the values are positive and most of the values are smaller that the average), and therefore it is far from the gaussian distribution. Furthermore, the AE time series is, as stated before, intermittent such that there are alternating bursts and quiet periods, while the FFT (Fast Fourier Transform) randomized time series is more homogeneous. However, the surrogate data method suggested by Theiler et al. (we use the method 2 in [Theiler et al., 1992]) preserves the amplitude distribution and intermittency. The surrogate time series looks very similar to the original time series, as is evident from Figure 12 where we show the AE time series of 5 days beginning on February 1, 1981 (Figure 12a), and its surrogate data (Figure 12b). This kind of surrogate data method tests a null hypothesis that the data corresponds to a static nonlinear transform of a linear stochastic process. The hypothesis breaks if the results for the surrogate data are very different from those for the original data.

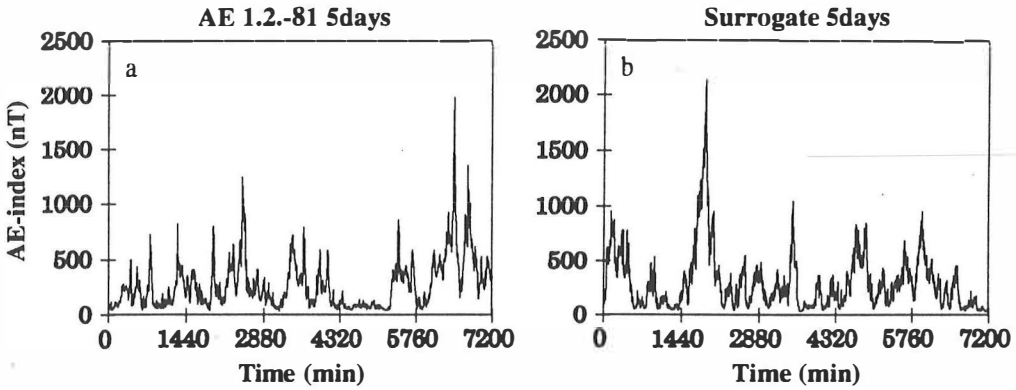

Figure 12. (a) The time series of the AE data of 5 days beginning on February 1, 1981. (b) The time series of the corresponding surrogate data.

In Figure 13a we show the slopes of the correlation sums for the original data of five days on February 1, 1981, and in Figure 13b those of the corresponding surrogate data with embedding values m=5,6,..,12 and a time lag of 20 min. The curves look very similar and the saturation is at a value between 3 and 4 for both sets of the slopes. The "hill" effect is even more pronounced for the original data. Qualitatively the behaviour of the slopes is similar, although the scaling region is longer, and the correlation dimension a little smaller, for the original data. However, as stated in Section 2.2, the results vary quite a lot between different periods of the AE data. Besides the average activity, also the proportion of quiet and active subperiods in the considered data sequence affects the slopes. This variation is caused by the nonhomogeneity of the time series which leads to nonuniformity of the density of points in the constructed state space. However, the null hypothesis that the data represents nonlinear filtering of a stochastic process seems to be valid in this case [Prichard and Price, 1993a; Prichard, 1993].

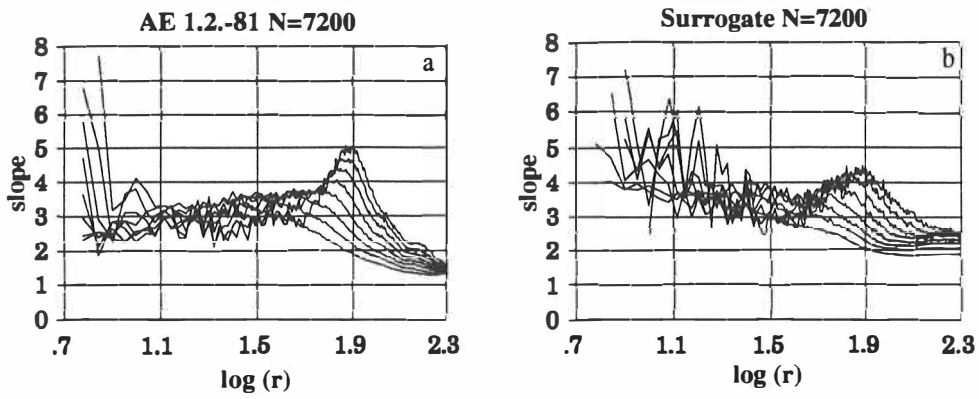

Figure 13. (a) Plots of the slopes of the GP correlation sum for the original AE data of Figure 12a. (b) Plots of the slopes for the surrogate data of Figure 12b. The results are calculated for m=5,6,...,12 (from bottom to top at log(r)=1.9), and for a time lag of 20 min.

3. Structure function

3.1. General

A linear method which is often used in time series analysis to distinguish between a deterministic signal of a strange attractor and stochastic noise is the structure function (SF). We define the SF [Mandelbrot, 1983; Osborne and Provenzale, 1989; Greis and Greenside, 1991; Takalo et al., 1993, 1994a and 1994c] by the expression

$$S(\lambda) = \langle |x(t_i + \lambda\,\Delta t) - x(t_i)| \rangle \quad , \tag{14}$$

where Δt is the sampling time, λ is an integer step, and $\langle |.| \rangle$ denotes an average of the absolute values. For fractal noise the structure function scales like

$$S(\lambda) \propto \lambda^H \tag{15}$$

for small values of λ. H is called a scaling exponent and we can find it by plotting the structure function versus λ on a log-log scale. If the plot is a straight line with a slope $0<H<1$, the signal is called self-affine. In this work we also study the scaling exponent H by considering the local slopes $d \log(S(\lambda)) / d \log(\lambda)$ between two adjacent points as a function of λ. For self-affine time series this should be constant at least for small values of λ.

3.2. Fractal (coloured) noise

It is known that for fractal noise with a power-law power spectrum, $P(f) - f^{-\alpha}$, one has $\alpha \approx 2H + 1$ [Panchev, 1971; Osborne and Provenzale, 1989; Voss, 1989; Provenzale et al., 1992; Takalo et al., 1994c]. It should be noted that this relation is true only within the range $1 < \alpha < 3$, and that it is not exact at the endpoints of this range. For $\alpha \approx 1$ for example, $H \approx 0.1$ [Osborne and Provenzale, 1989]. In Figure 14a we show the SF for 262144 points of coloured noise with $\alpha = 2$ (upper curve). The scaling exponent H is almost exactly 0.5, in complete agreement with the theory, up to 500 time steps. There are some fluctuations at greater values of λ, as can be seen from Figure 14b (upper curve) where we show the slopes $d \log(S(\lambda)) / d \log(\lambda)$ of the SF of Figure 14a. These fluctuations result from decreasing autocorrelation with increasing λ. In Figure 14a we also plot the SF of our bicoloured noise (lower curve) which is designed to resemble the AE data [Takalo et al. 1993 and 1994a]. Bicoloured noise is coloured noise such that the spectral exponent changes at a critical frequency. In this case we use $\alpha = 2$ for high frequencies and $\alpha = 1$ for low frequencies, and the spectral exponent changes at a critical frequency of $f_c = k_c/N = 1/300$. We have plotted here the SF of little over 300000 points of bicoloured noise [Takalo et al., 1994c]. The scaling exponent is about H=0.5 for small values of λ, and decreases then slowly to a value of about 0.15 on the average. In Figure 14b we show the local slopes of the SF of the AE data (lower curve). It is evident from this figure that the scaling exponent changes at a time scale which is about a half of the critical period in the power spectrum [Takalo et al. 1993 and 1994c; Takalo and Timonen 1994]. The crossover region where the scaling exponent changes is quite broad, but it is only natural in this kind of phenomena [Higuchi, 1990; Greis and Greenside, 1991].

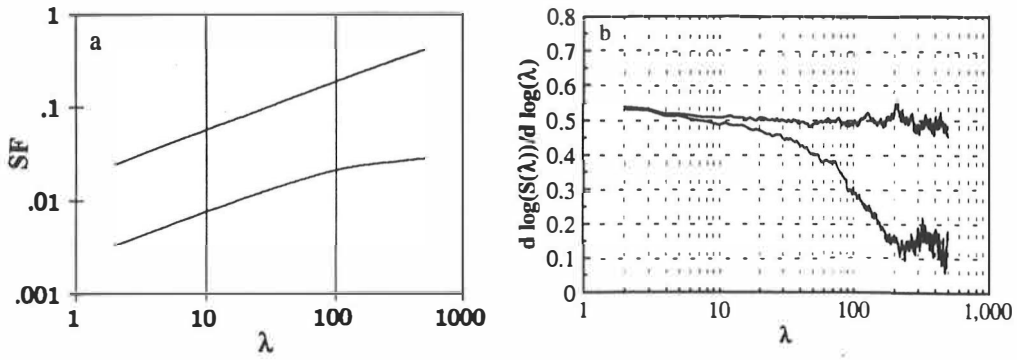

Figure 14. (a) Structure function of coloured noise with spectral exponent $\alpha = 2$ (upper curve) and that of bicoloured noise with $f_c = 1/300$ (lower curve). (b) The plots of the slopes of the two SFs of Figure 14a (Figure 14b from Takalo et al., [1994c]).

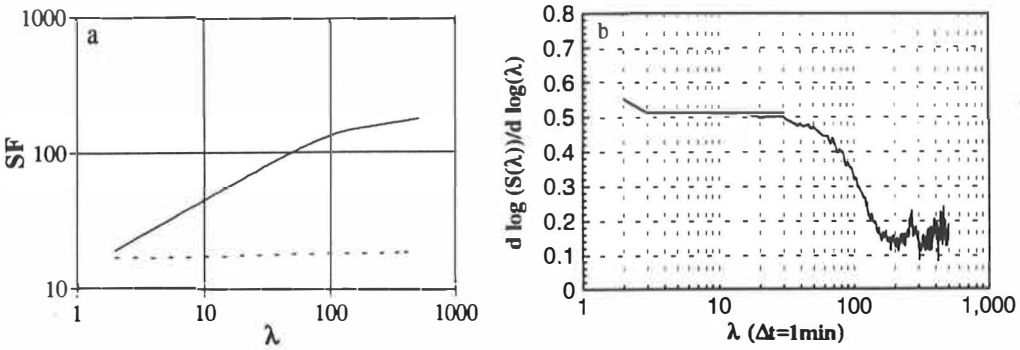

Figure 15. (a) Structure function of the AE data (solid curve) and of the differenced AE data (dotted curve) for the data of year 1985. (b) Plot of the slopes of the SF for the AE data of Figure 15a (Figure 15a from Takalo et al., [1994a], Figure 15b from Takalo et al., [1994c])

3.3. AE and AL data

We have shown before that the SFs of AE data [Takalo et al., 1993 and 1994a] and AL data [Takalo et al., 1994b] are very similar to that of bicoloured noise. Here we only plot in Figure 15a the SF of the AE data for 1985 as a function of λ(solid curve). It is evident that the slope for small values of λ is almost exactly 0.5, and then decreases to about 0.15 on the average. There is also quite a broad crossover region, where the change in the slope takes place. This can be seen in Figure 15b, where we show the local slopes for the SF of Figure 15a. We have made a fourth order polynomial fit to the curve of the slopes of the SF for the years 1978-85, and find that the inflection point is at 113 minutes with a standard deviation of 9 minutes. We may say therefore that the time scale at which the scaling exponent H changes is 113 (±9) minutes [Takalo et al, 1994c]. The scaling exponent H is H=0.5 for times shorter than 113 min and is therefore the same as that of coloured noise with spectral exponent $\alpha = 2$.

In Figure 15a we also show the SF of the differenced time series of the AE data for 1985 (dotted curve). The scaling exponent H is $H \approx 0$, and there is hardly any structure in the time series. However, in the case of differenced data of a strange attractor, there should be some residual structure in the SF [Takalo et al, 1994b] as shown in the next Section 3.4. In contrast with this, the differenced AE data is nearly white noise [Takalo et al., 1994a].

3.4. Strange attractor

The structure function of the Lorenz attractor (Figure 16a, solid curve) displays a behaviour which is totally different from that of the AE data or bicoloured noise. The structure function is periodic having a minimum after about every 69 timesteps [Takalo et al., 1994a]. This property follows from close returns of the trajectory after about every 69 steps when a time increment of 0.01 s is used and the cofficients of the Lorenz attractor are σ=10, r=28, b=8/3 ($\dot{x} = \sigma(y-x)$, $\dot{y} = x(r-z)-y$, $\dot{z} = xy-bz$). The plot of the local slopes of the SF of the Lorenz attractor (Figure 16b) shows that the scaling exponent approaches asymptotically 1 when $\lambda \rightarrow 0$. This is a property of all smooth differentiable curves. The periodicities of a time series can be seen from the local slopes of the SF by noticing that the maxima and minima of the SF correspond to points where the local slope vanishes. The structure function of the differenced time series of the Lorenz attractor (Figure 16a, dashed curve) looks quite the same as that of the original time series, while the structure function of the differenced AE data is perfectly flat.

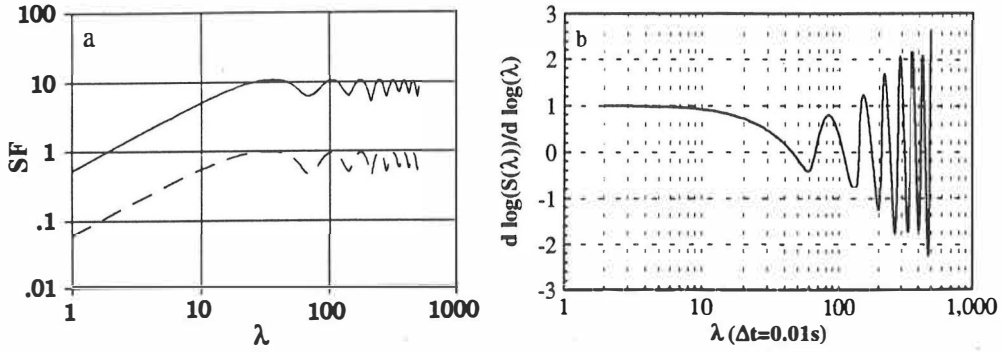

Figure 16. (a) Structure functions of the Lorenz attractor (solid curce) and its differenced attractor (dashed curve). (b) Plot of the slopes of the SF for the Lorenz attractor (Figure 16a from Takalo et al., [1994a], Figure 16b from Takalo et al., [1994c]).

3.5. Dst data

The SF is conventionally used to study the self-affinity of the time series. However, as already seen in the SF of the Lorenz attractor, it may also reveal periodicities inherent in a time series. The SF of the Dst data as a function of λ(Figure 17a) shows that, although the slope for small values of λ starts at a value of about 0.5 in the same way as that of the AE data, it decreases very quickly. This is better seen from the local slopes of the SF of Figure 17a (Figure 17b). There does not seem to be any clear scaling region where the slope should

stay constant. Instead the slope seems to be periodic such that there is a minimum after every 24 hours.

To be more precise, one period is at the point where the slope vanishes after a minimum. For small values of λ the slope is always positive, and the period can be identified as the point where the slope begins to increase after a minimum. From this plot we can easily see that there is a diurnal period in the SF of the Dst data. There also seems to be fine structure inside this 24-hour period. We have shown that there are also other periodicities in the AE data which can be found by a detailed analysis of the SF function [Takalo et al., 1994c].

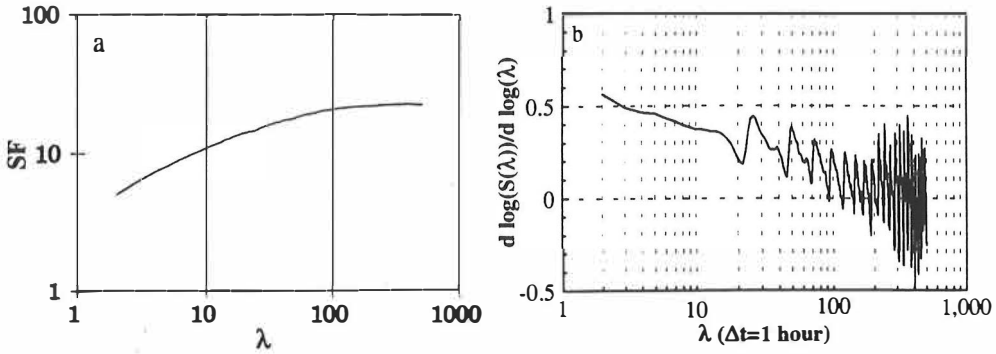

Figure 17. (a) Structure function of the Dst data of the years 1957-84. (b) Plot of the local slopes of the SF in Figure 17a.

3.6. Connections between ACF, SF and the power spectrum

A connection between the SF and the ACF can be derived by starting from the scaling property [Takalo and Timonen, 1994]

$$\langle [x(t+\lambda\Delta t)-x(t)]^2 \rangle = \lambda^{2H} \langle [x(t+\Delta t)-x(t)]^2 \rangle \ , \tag{16}$$

and assuming that the time series is self-affine (here and in the following discussion equality means that in the statistical sense). From this expression we can deduce a similar scaling property for the normalized ACF [Takalo and Timonen, 1994] (See also [Panchev, 1971; Burlaga and Klein, 1986]):

$$1 - AC(\lambda\Delta t) = \lambda^{2H} [1 - AC(\Delta t)] \ . \tag{17}$$

We show in Figure 18b the plot of expression $[(1-AC(\lambda\Delta t))/(1-AC(\Delta t))]^{1/2}$ as a function of λ on a log-log scale as calculated from the ACF of 100 days (144000 points) of the AE data (Figure 18a) beginning on January 1, 1983. The curve is indeed quite straight up to approximately 115 min with a slope $H \approx 0.5$. Of course the change in the slope around 115 min is not sharp but there is again a smooth crossover region. It is evident that the curve of Figure 18b is compatible with the SF of Figure 15a. On the other hand, the power spectrum of the data is the Fourier transform of its ACF. In Figure 18c we show the power spectrum of the AE data as calculated from the ACF of Figure 18a. The power spectrum of Figure 18c is

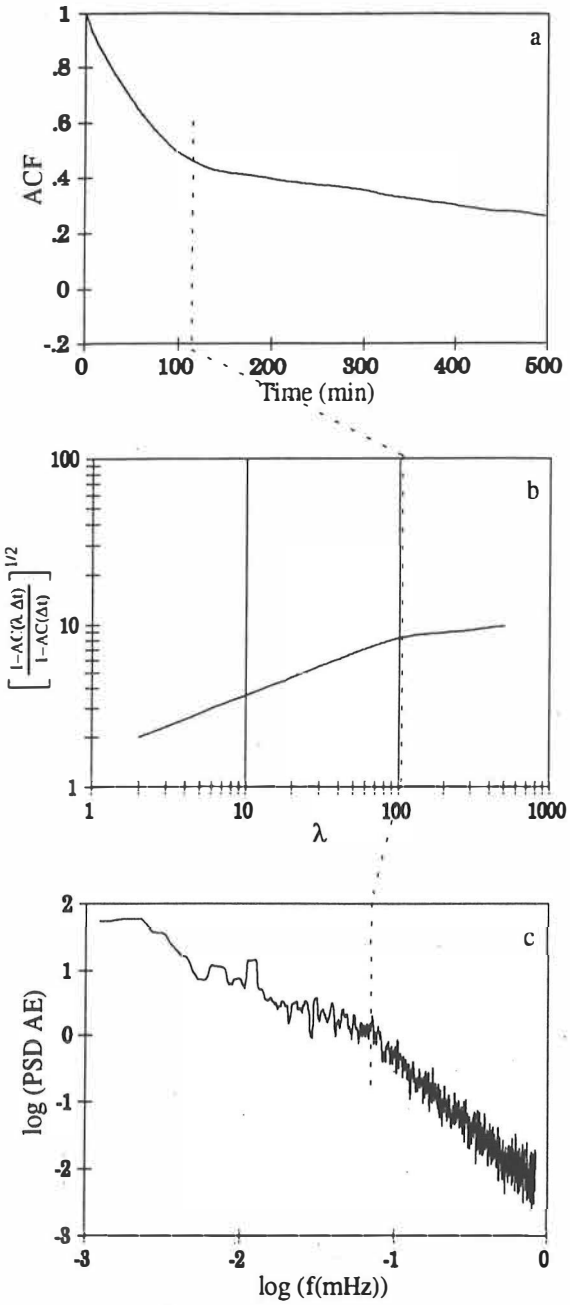

Figure 18. (a) Autocorrelation function (ACF) of 100 days of the AE data beginning on January 1, 1983. (b) The scaling function as calculated from the ACF of Figure 18a. (c) The power spectrum of the AE data as calculated from the ACF of Figurel 8a. The dotted line shows the relation between the time scales of the different figures (from Takalo and Timonen [1994]).

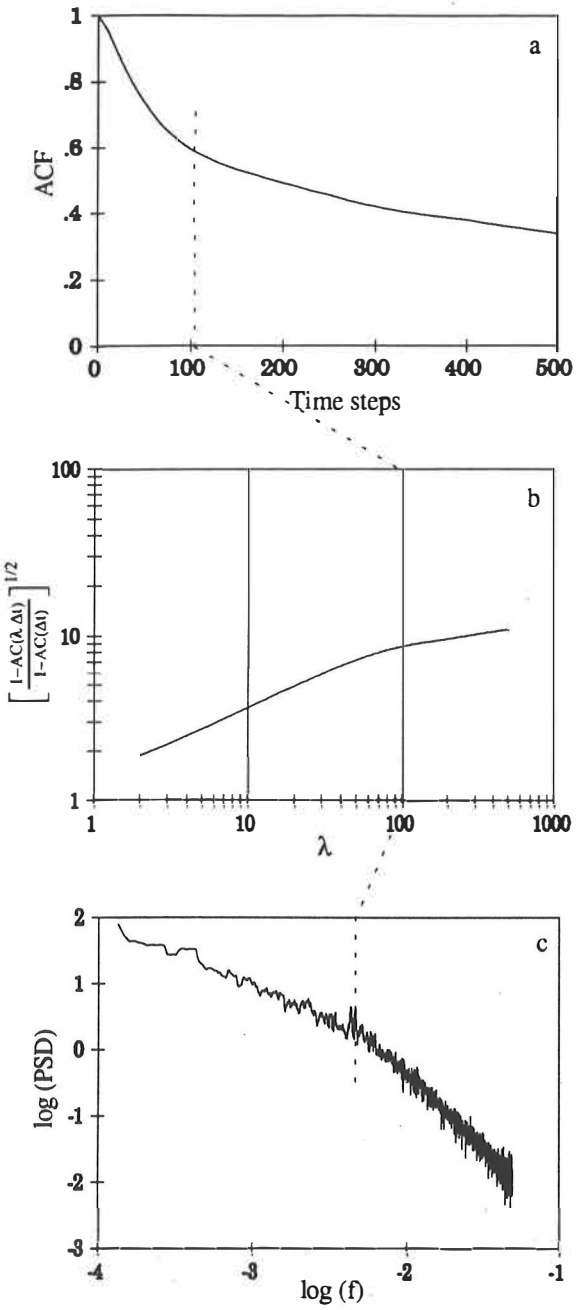

Figure 19. (a) ACF of about 100000 points of bicoloured noise with a critical frequency of f_c=1/200. (b) The scaling function as calculated from the ACF of Figure 19a. (c) The power spectrum of bicoloured noise as calculated from the ACF of Figure19a.

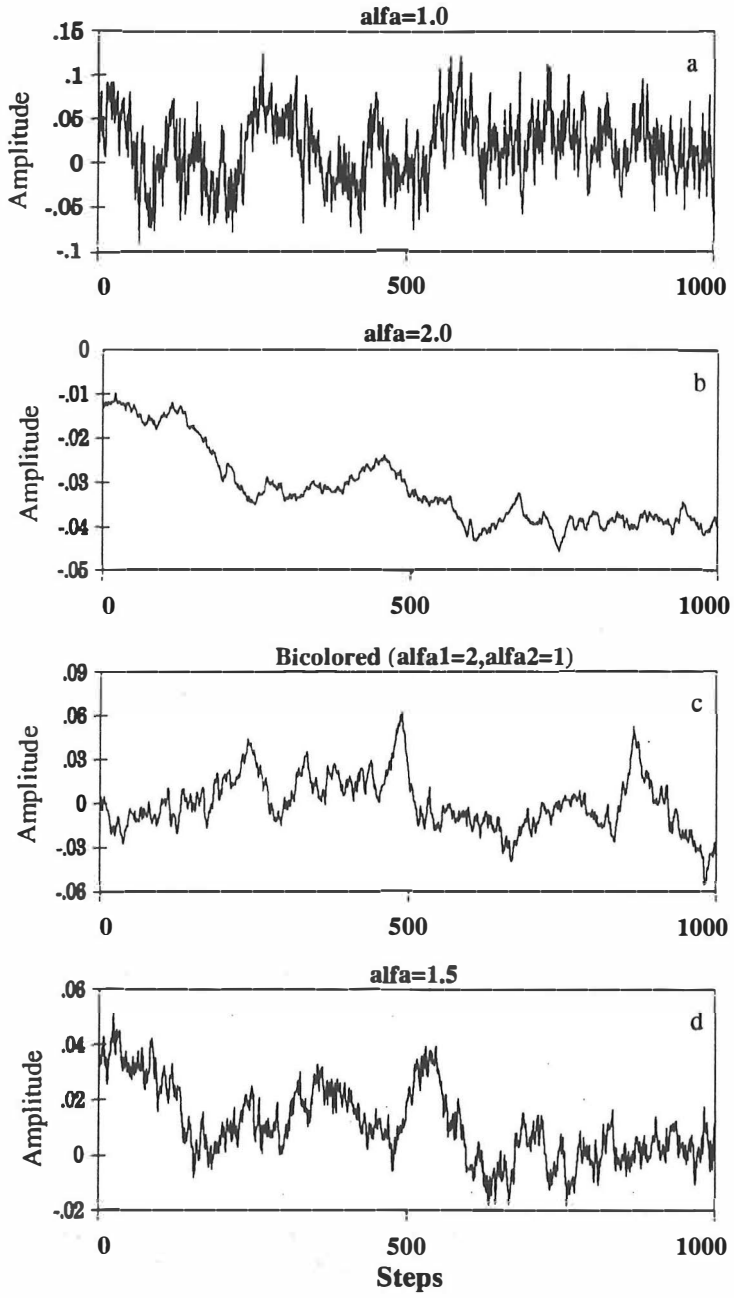

Figure 20. Time series of coloured noise with different spectral exponents.

very typical of the AE data with a slope $\alpha = 1.01$ for low frequencies, and with $\alpha = 2.01$ for high frequencies. The break in the power spectrum here is at a frequency of $6.7 * 10^{-5}$ Hz (about 250 min period). We interpret this result such that there is a connection between the time scale of approximately 115 minutes in the SF and in the ACF of the AE data [Takalo and Timonen, 1994, Takalo et al., 1994c], and the break at a period of approximately 300 minutes in the power spectrum of the AE data [Tsurutani et al., 1990; Takalo et al., 1993, Takalo and Timonen, 1994; Takalo et al., 1994c]. It is well-known that, if we take samples from a time series at 2 hr. intervals, the highest frequency we get in the data is 1/(4hr.) (Nyquist frequency, see e.g. [Brigham, 1974; Priestley, 1981]). In other words when the properties of a time series change at some time scale, the critical period in the power spectrum of the time series corresponds to twice that time scale.

As a further evidence of the connection between the time and frequency scales, we have generated noise with two colours, i.e. bicoloured noise [Takalo et al., 1993 and 1994a] such that for frequencies below e.g. $f_c = 1/200$ the spectral exponent is $\alpha = 1$, and for $f > f_c$ it is $\alpha = 2$ (see power spectrum in Figure 19c). The ACF calculated from about 100000 points of this bicoloured noise is shown in Figure 19a. It is evident that nothing particular happens at the period of 200 time steps. On the other hand there is a clear change in the ACF at a time scale of 100 time steps from an exponential decay to a linear decay (see Section 4.1). Figure 19b shows the scaling plot of bicoloured noise as calculated from the normalized ACF of Figure 19a. The scaling exponent seems to change at about the time scale of 100 time steps with slopes similar to those of the AE data, and the crossover region is even broader than that for the experimental AE data. However, also in this case of bicoloured noise the autocorrelation time (as defined in Section 4.1) equals the time scale at which the scaling properties change, and this time scale is connected to a critical period at twice that time scale in the power spectrum.

As a concrete example of the change of the scaling properties we visualise in Figure 20 coloured noise, ($P(f) \propto f^{-\alpha}$), for a few different spectral exponents. In Figure 20a we show coloured noise with $\alpha = 1$. This time series is clearly more rapidly changing than that of the AE data (when considered such that one step here corresponds to one min sampling time for the AE data). In Figure 20b we show coloured noise with $\alpha = 2$. The time series is varying much more slowly, and, if there is a deviation from zero, it takes a long time for the curve to return close to zero. The autocorrelation time of this time series is consequently very long (time series describes Brownian motion and consecutive points in the series are correlated). However, if one combines these two different kinds of coloured noise such that the spectral exponent is $\alpha = 1$ for low frequencies and $\alpha = 2$ for high frequencies, one finds the curve shown in Figure 20c. The spectral exponent changes at a critical frequency of 1/200. The curve is very similar to that of Figure 20b at small time scales (up to about 100 time steps), and there are no big sudden changes in the curve at short times. However, at longer times the curve is not so smooth (it scales similarly to that in Figure 20a), and there are big changes at time scales longer than about 100 time steps. In Figure 20d we show (mono)coloured noise with the spectral exponent $\alpha = 1.5$ (mean of those relevant for Figures 20a and 20b). The curve is clearly more irregular at small scales than that of bicoloured noise of Figure 20c. Some authors [Roberts, 1991; Pavlos et al., 1992] have erroneously compared the properties of the AE and AL indices to those of monocoloured noise, while the original data clearly has a power spectrum which contains two "colours".

4. Other methods

4.1. Autocorrelation function

Recently autocorrelation times or related quantities have been used to define the time lag in the embedding dimension analysis of the AE and AL data [Shan et al., 1991a, 1991b; Roberts et al., 1991; Vassiliadis et al., 1991; Takalo et al., 1993, 1994a]. Determination of the proper autocorrelation time for the AE and AL data is difficult because of the nonstationarity of these data [Prichard and Price, 1993b; Takalo et al., 1994a]. Nonstationarity means that the statistical properties of the data change with time. One property of a nonstationary time series is that its autocorrelation time increases with increasing number of data points. This kind of behaviour can in fact be seen in the Figure 21 where we show the ACFs of 5-, 20-, 100-, and 200-day periods of the AE data beginning on January 1, 1983. It is evident that the ACF decays more slowly with increasing number of data points.

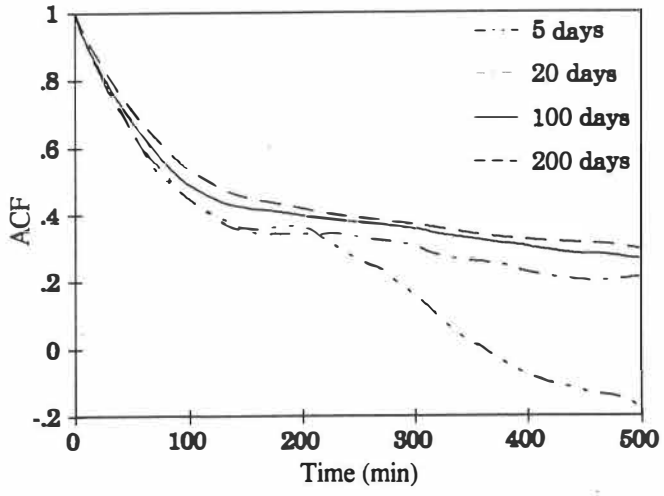

Figure 21. Autocorrelation functions for 5-day, 20-day, 100-day, and 200-day periods of the AE time series beginning on January 1, 1983 (from Takalo and Timonen, [1994]).

Because of the difficulties inherent in the conventional definitions of the autocorrelation time, we shall define it as the break in the ACF such that for times before the break the ACF decays exponentially. For times greater than the break the ACF is roughly linear, which means that a kind of plateau sets in in the ACF. Although the ACF decays more slowly with increasing number of data points, and the plateau in the ACF appears at a higher level, the onset of this plateau is almost independent of the length of the time series. It is evident from Figure 21 that the plateau sets in at approximately 120 minutes for all these time series [Takalo and Timonen, 1994].

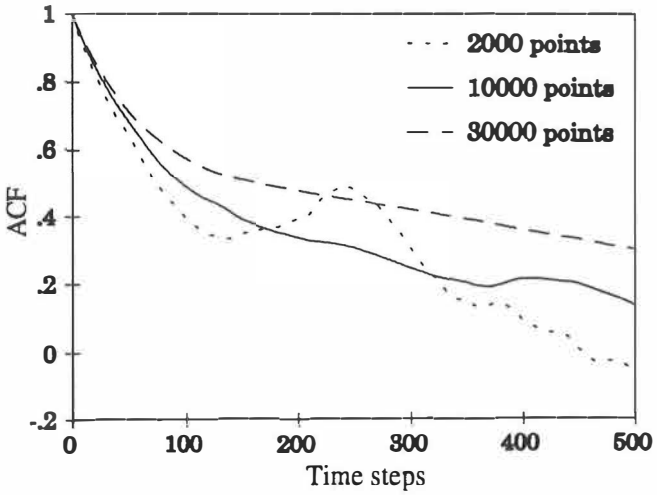

Figure 22. Autocorrelation functions of 2000, 10000 and 30000 points of bicoloured noise with a critical frequency of f_c=1/200.

It should be noted that nonstationarity is also a property of coloured noise. Nonstationarity arises because the power spectrum of coloured noise is proportional to $f^{-\alpha}$, and hence the dominant period is always of the order of the length of the time series [Meyer-Kress, 1988; Theiler, 1991]. This is obvious from Figure 22 where we show the ACFs for 2000, 10000, and 30000 points of bicoloured noise with a critical frequency of 1/200. The decay time clearly increases with increasing number of data points. Also, peaks in the ACF which result from singular features in the time series, are clearly seen in the 2000-point curve but disappear when the number of data points is increased. Notice the similarity between the ACFs of Figure 21 for the AE data and that for bicoloured noise shown in Figure 22. It seems that tens of thousands of points are needed for a proper ACF of bicoloured noise. However, because the AE data is more inhomogeneous than bicoloured noise, of the order of hundred thousand points are needed for a proper ACF of the AE data [Prichard and Price, 1993b].

In Figure 23 we show the ACFs for coloured noise with different spectral exponents. While the ACF of coloured noise with $\alpha = 1$ decays very quickly, those of coloured noise with spectral exponents 1.5 and 2 decay very slowly. However, for bicoloured noise with spectral exponent $\alpha = 1$ for low frequencies and $\alpha = 2$ for high frequencies (f_c=1/200), the behaviour is totally different. The ACF first decays exponentially for time scales shorter than 100 time steps (half of the critical period in the power spectrum [Takalo and Timonen, 1994]). Then a kind of plateau sets in in the ACF, and the decay becomes roughly linear. It is instructive to compare the ACFs of Figure 23 to their respective time series shown in Figure 20. Pavlos et al. [1992] have erroneously compared the ACF of the AE data to that of monocoloured noise. That is why they find ACFs similar to those for $\alpha = 1.5$ and $\alpha = 2$ in Figure 23.

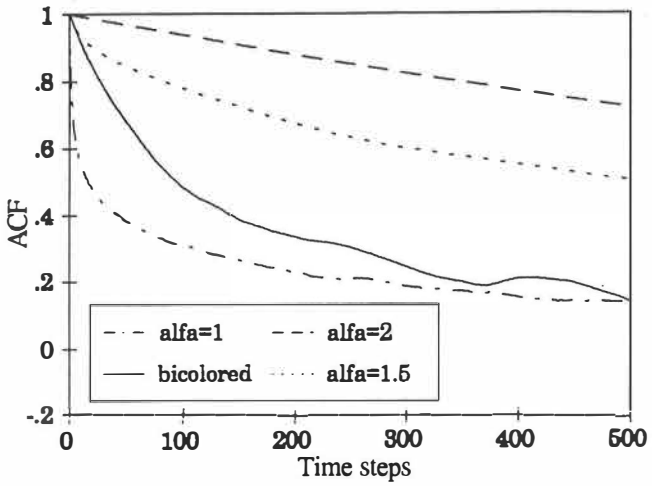

Figure 23. Autocorrelation functions of coloured noise with different spectral exponents (see Figure 20 for the corresponding time series).

4.2. Recurrence plot

Recently a method called recurrence plot has been used as a diagnostic tool in analysing the data of dynamical systems [Eckmann et al., 1987; Zbilut and Webber, 1992; Koebbe and Mayer-Kress, 1992]. The method is the following: Let x(i) denote the i-th point in an m-dimensional state space for i=1,..,N. Construct an $N \times N$ array such that a dot is marked at point (i,j) when the distance is $|x(i) - x(j)| \leq r$ in the state space. The radius r is chosen arbitrarily but kept fixed such that enough points are found for the fine structure of the plot. We have applied this method to the analysis of the AE time series [Takalo et al, 1994a].

In Figure 24a we show the recurrence plot of the AE time series of 1000 points for the period beginning on January 1, 1983. The plot is made for embedding dimension m=9 with a time lag of 50 minutes. It is symmetric with respect to the diagonal as it should be. The most visible feature of the plot is that nearby points in the state space are also close in time because the data are highly autocorrelated. This is why Theiler [1986] proposed a method for omitting these nearby points, which produce "knees" in the correlation integral and lead to spurious estimates for the dimension. In Figure 24b we show the recurrence plot for bicoloured noise with m=9 and a time lag of 50 time steps. The structure of the plot is quite similar to that of the AE data. In both figures there are points scattered around the diagonal. This suggests that the trajectory is folded locally which causes fractal behaviour along the trajectory. On the other hand, quite a different behaviour can be seen in Figure 24c which shows the recurrence plot of the Lorenz attractor with a lag of 10 time steps. There are lines parallel to the diagonal which shows that a part of the trajectory, say x(j), x(j+1),..., x(j+k), comes close to an earlier part of the trajectory, x(i), x(i+1),..., x(i+k). The length of the lines is proportional to the inverse of the largest positive Lyapunov exponent [Eckmann et al., 1987].

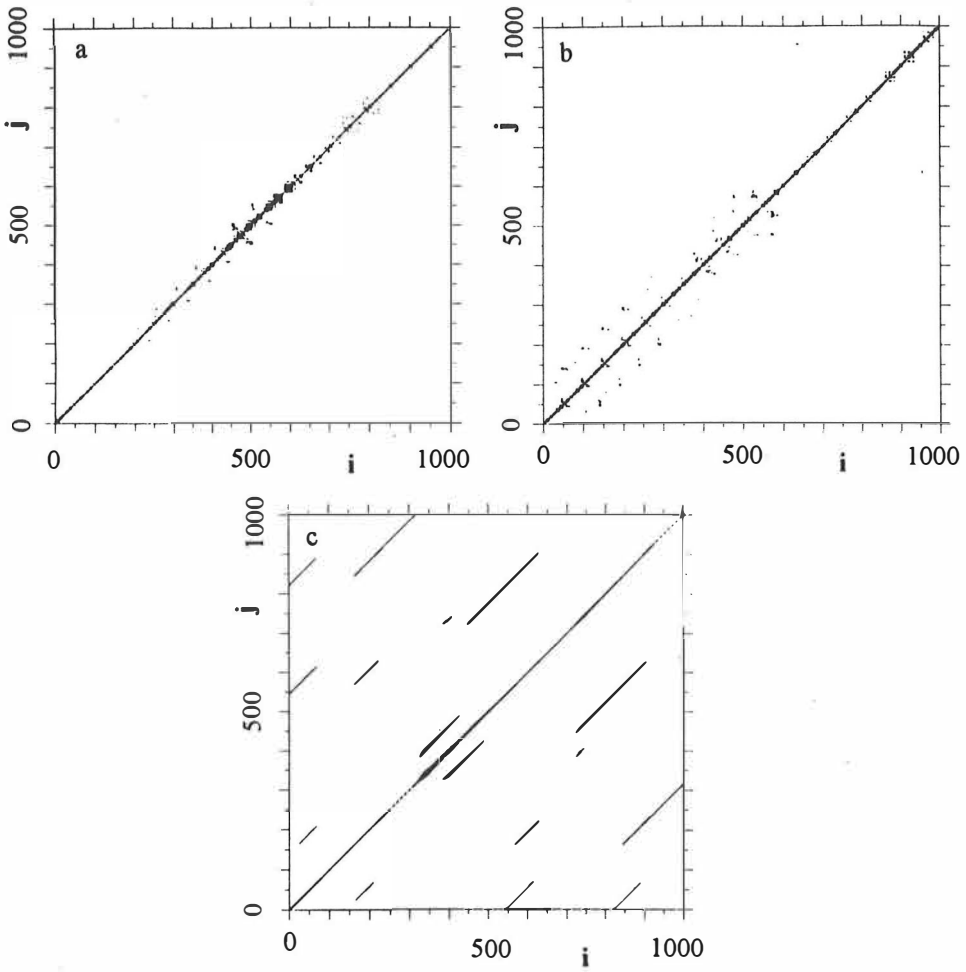

Figure 24. Recurrence plots of (a) AE data for the period beginning on January 1, 1983, (b) bicoloured noise, and (c) Lorenz attractor (from Takalo et al.,[1994a]).

4.3. A test for determinism in time series

Different methods have also been developed for determining the extent to which determinism can explain the behaviour of a time series [Sugihara and May, 1990; Kaplan and Glass,1992; Wayland et al., 1993]. We shall report here an application of the last one of these methods [Takalo et al., 1994a]. In order to diminish the possible effect of autocorrelation, we shall analyse the differenced time series of the AE data and of bicoloured noise, and compare the results with those for the Hénon [Hénon, 1976] and Lorenz [Lorenz, 1963] attractors. The method is the following [Wayland et al., 1993]: Let x_o be an arbitrary center point in the state space. Find the k nearest points $x_1, ..., x_k$ to x_o. Let now $y_o, ..., y_k$ denote the images of these points ($y_i = x_{i+\tau}$), and construct the translation vectors $v_i = y_i - x_i$. From these vectors calculate the translation error

$$e_{tr} = \frac{1}{k+1} \sum_{i=0}^{k} \frac{|v_i - \langle v \rangle|^2}{|\langle v \rangle|^2} \quad , \tag{18}$$

where $\langle v \rangle$ is the average of the translation vectors. The final translation error $\langle e_{tr} \rangle$ is calculated as an average over N_c center points. The idea of this method is that, if the time series is deterministic, the translation vectors will be rather similar and hence the translation error will be small. Notice that the translation error is normalized by dividing by $|\langle v \rangle|^2$, and so e_{tr} should be independent of the overall scaling of the time series.

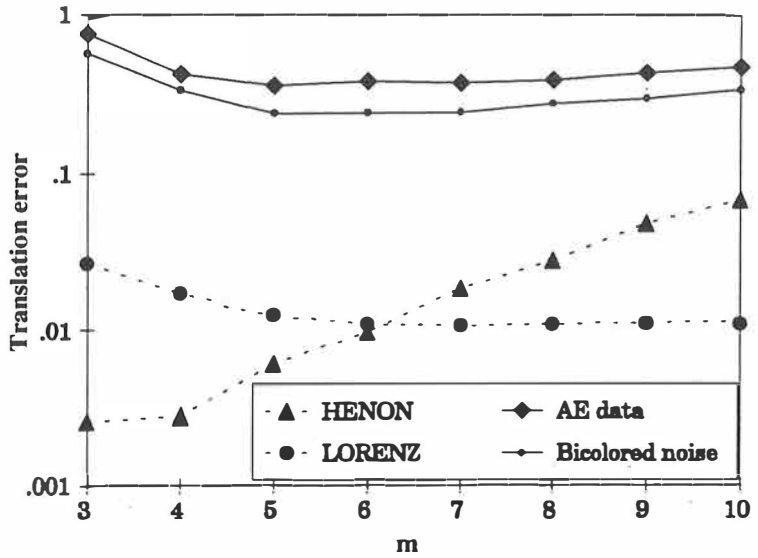

Figure 25. Translation errors as a function of the embedding dimension for differenced AE data (April 1, 1983) and differenced bicoloured noise. For comparison the translation errors for the Henon and Lorenz attractors are also shown (from Takalo et al., [1994a]).

In Figure 25 we show the average translation errors as a function of embedding dimension for the differenced AE data (April 1, 1993) with $N = 7200$, $N_c = 700$, and a time lag of 5 time steps, and for differenced bicoloured noise with the same parameter values. The image points are chosen such that $y_i = x_{i+5}$. For comparison, we show in this figure the corresponding results for the Henon attractor with coefficients 1.4 and 0.3 (N=4096, N_c=400, time lag = 2), and the Lorenz attractor with coefficients 10, 28 and 8/3 (N=4096, N_c=400, time lag = 5). Our results for these two attractors are compatible with those of Wayland et al. [1993]. Figure 25 clearly indicates that the translation error curves for the differenced AE data and differenced bicoloured noise differ substantially from those for the two deterministic attractors.

However, if we calculate the translation error from the original data by using image points far from the initial points, the AE time series may appear more deterministic than bicoloured noise. We show in Figure 26 the results for two different periods of AE data for which the image points are chosen such that their separations from the initial points are larger than the autocorrelation distances, namely $y_i = x_{i+150}$. The quiet period of the AE data begins on January 8, 1979, the active period begins on April 1, 1983, and all translation errors are

calculated with N=7200 and a time lag of 40 time steps. For small values of the embedding dimension m, all data appear stochastic, but the translation errors of the AE data decrease with increasing m, and more so for the active period. Notice that bicoloured noise also appears more "deterministic" than pure white noise, and its translation error behaves for increasing embedding dimension very much like that of the AE data. So there is again similar behaviour between AE data and bicoloured noise.

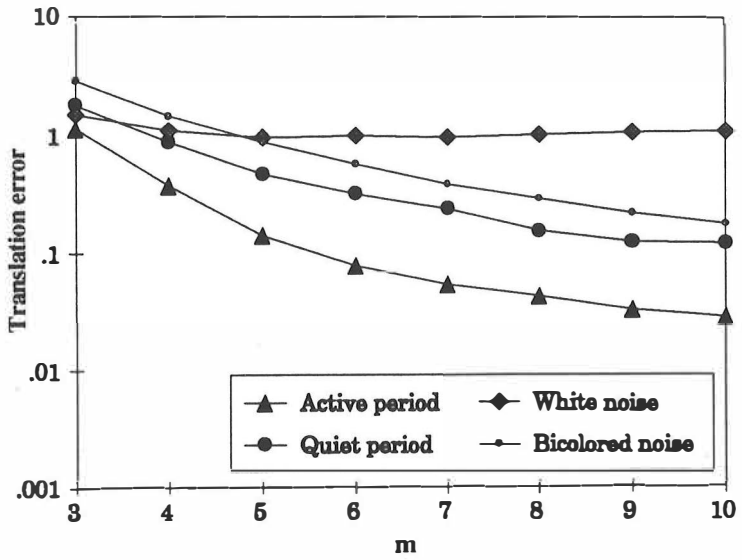

Figure 26. Translation errors for four different time series. The active period of the AE data is from the beginning of April 1983, and the quiet period begins on January 8, 1979 (from Takalo et al., [1994a]).

4.4. Phase-angle distribution

We have shown before [Takalo et al., 1994] that the power spectra of the AE data and of the Lorenz attractor differ essentially from each other. If the signal of a deterministic dynamical system is n times differentiable, its power spectrum falls off faster than f^{-2n}. In general the variables of mathematical attractors (like those of the Lorenz attractor) are infinitely times differentiable and thus their power spectra decay at high frequencies faster than any power of f^{-1}, i.e. they must decay exponentially [Sigeti and Horsthemke, 1987].

A better way to distinguish between differentiable and stochastic dynamics at high frequencies is perhaps to study the phase-angle distribution of the complex Fourier transform of the time series [Osborne and Pastorello, 1993]. In Figure 27a we show the phase-angle distribution of Lorenz attractor. The phases are random at low frequencies, but at high frequencies there appears phase-locking due to differentiable dynamics. This is connected to the rapid decay of spectral weight at high frequencies of the Lorenz attractor [Osborne and Pastorello, 1993; Takalo et al., 1994a]. In Figure 27b we show a typical phase-angle distribution for the AE data. It is evident that the phases are totally random. However if the sampling time of the considered time series is too long we may loose the features related to phase-locking. Because the resolution of the AE data is 1 minute, we have also studied data

from Muonio (northern Finland) and Söröya (northern Norway) magnetometers. Although the resolution of these data is 20 seconds, we did not find any phase-locking in them and their phase-angle distributions were random.

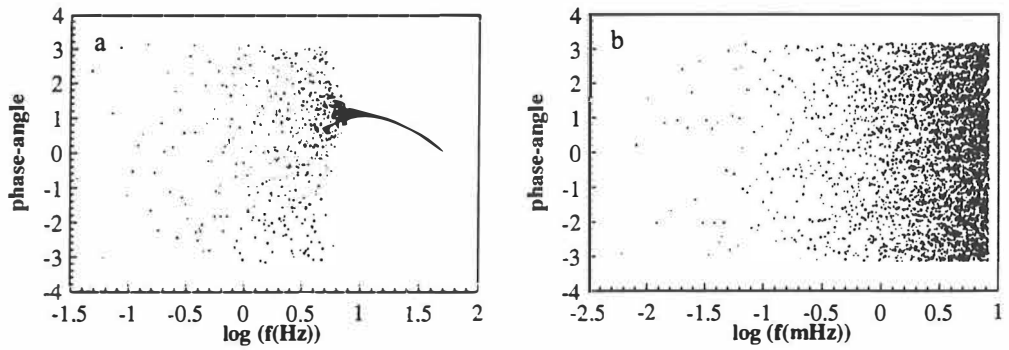

Figure 27. (a) Phase-angle distribution of a time series of the x-component of the Lorenz attractor. (b) Phase-angle distribution of the AE data beginning on January 1, 1983. Both figures consist of 4096 points.

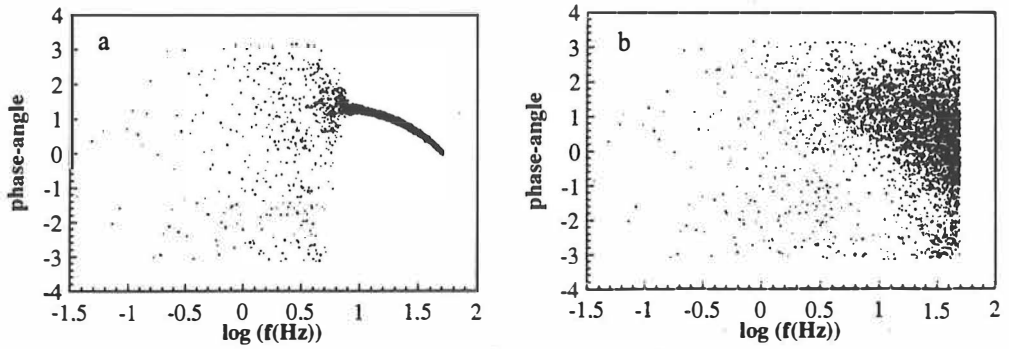

Figure 28. (a) Phase-angle distribution of the x-component of the Lorenz attractor with an added 5% of coloured noise with $\alpha = 2$. (b) Same as (a) but with an added 5% of coloured noise with $\alpha = 1$.

However, quite a small amount of noise may destroy the phase-locking at high frequencies. The amount of noise needed for that depends upon the power spectrum of the noise. We have added different types of coloured noise to the time series of the x-component of the Lorenz attractor such that the new time series is

$$y(t_k) = x(t_k) + \delta(t_k) , \qquad (19)$$

where $\delta(t_k)$ is a time series of power-law (coloured) noise whose power spectrum behaves like $f^{-\alpha}$. This kind of noise seems to be very usual in nature. In Figure 28a we show the data of the Lorenz attractor with 5% (as calculated from the standard deviation) of added coloured noise with $\alpha = 2$. It is evident that the phase-locking is still clearly visible although the angle

distribution appears to be broadened. However, with the same amount of added coloured noise with $\alpha = 1$, the signs of phase-locking have completely disappeared (Figure 28b). For small values of the spectral exponents α there is more spectral weight at higher frequencies and noise affects more the dynamics at those frequencies. The amount of noise needed to totally destroy the phase-locking at high frequencies is found to be approximately 40% for $\alpha = 2$, 4% for $\alpha = 1$, and only about 1% for "white" noise with $\alpha=0$, as calculated from their standard deviations.

5. Conclusions

This work divides roughly into three different parts: the possible existence of an attractor in the dynamics of the magnetosphere, the characteristic time scale of the auroral electrojet data, and the use of structure function in the analysis of the magnetospheric time series.

We find that the correlation dimension of the AE time series is 3.4 on the average. We also find indications of the correlation dimension to depend weakly on the geomagnetic activity such that it decreases with increasing activity. However, the results for bicoloured noise show that it also has a low correlation dimension, and the slopes of the correlation sums are very much like those of the AE data. Furthermore, the slopes of the GP correlation sums for the surrogate data [Theiler et al., 1992] are similar to those for the original data. These facts suggest that the low correlation dimension is, at least partly, a consequence of the AE data being a nonlinear transform of some linear stochastic process.

We have also used differentiation of the data in our correlation dimension analysis. Some of the result show that the differenced AL data also have a low correlation dimension. However, the saturation values differ appreciable from each other, and also from those of the original data. Furthermore, differentiation means one more filtering for the data, and it is well known that filtering of the data may produce apparent low-dimensional behaviour [Grassberger et al., 1991; Rapp et al., 1993; Vassiliadis and Daglis, 1993]. It has also been shown [Prichard, 1993] that differentiation moves the nonstationarity in the mean of the original data to nonstationarity in the variance of the differenced data. The low correlation dimension of the differenced data may thus be caused by nonuniformity of the points in the state space [Grassberger et al., 1991; Prichard, 1993].

We have also used several other methods of time series analysis to find whether the behaviour of the AE data would support the idea of the magnetospheric activity to exhibit low-dimensional deterministic features. In comparison of the properties of the AE data with those of bicoloured noise and with two standard fractal attractors, the Lorenz and the Henon attractor, different methods seem to point to the same direction: the properties of the AE data are qualitatively much more similar to those of bicoloured noise than to those of the attractors. This does not of course rule out the possibility that low-dimensional behaviour can eventually be found such that its dynamical properties would be more similar to those of the AE data than to those of well-known attractors. On present evidence we believe, however, that most probably the AE time series can be described as bicoloured noise or possibly another kind of fractal noise with similar characteristics.

Although the methods adopted in this work have generally been applied in studying experimental time series, there is a possible caveat in these methods. Magnetosphere is not an autonomous system but is continuously driven by the stochastic solar wind. It is therefore possible that, even if the magnetosphere were a low-dimensional chaotic system, we might not find it by studying just one time series. This is because the magnetosphere may not have time enough to converge to a possible attractor for times long enough to produce data with a detectable number of close returns of the trajectory. For this reason it has been suggested that the magnetosphere should be described as a nonlinear input-output system [Prichard and Price, 1992; Price and Prichard, 1993]. In order to resolve these intriguing problems, further analysis in this direction is clearly needed.

One of the basic questions is the smoothness of the data when using embedding method. It is usually assumed [Takens, 1981] that the time series used in the state space construction must be at least twice (maybe infinitely many times) differentiable. This requirement is not

fulfilled by the AE and AL data, because our results in the SF analysis show that these time series are self-affine fractals, and thus are not differentiable. Furthermore, our phase-angle distribution studies show that there is no differentiable dynamics to be found from these data.

We have shown that the AE data have a characteristic autocorrelation time, if properly defined, of approximately 120 minutes (118 ±9 minutes). The structure function of the AE data shows that the scaling properties of the AE time series change, within the error limits, at about the same time scale. For times shorter than 113 (±9) minutes the AE data have a scaling exponent H=0.5 which is similar to that of coloured noise with spectral exponent $\alpha = 2$. We have also shown that the scaling properties of the AE data can be directly derived from the autocorrelation function. This autocorrelation time is a kind of memory of the system. It is interesting to note that the typical duration of the auroral substorms is also about 2-2.5 hours [Bargatze et al., 1985; Baker et al., 1986]. It is evident that when a disturbance is once initiated, its typical duration equals the autocorrelation time of the system.

We also suggest that the break in the power spectrum of the AE data at the period of approximately 300 minutes is due to the characteristic autocorrelation time of approximately 120 minutes which is about half of the critical period in the power spectrum. This in turn is related to the change of the scaling properties of the AE data at about the same characteristic time scale. It seems that the low-frequency part of the power spectrum ($\alpha \approx 1$) mainly arises from the turbulent driving by the solar wind which has a similar power spectrum [Tsurutani et al., 1990; Feynman and Ruzmaikin, 1993], whereas the high-frequency part ($\alpha \approx 2$) is more intrinsic to the magnetosphere.

Conventionally the SF has been used to study the affinity of time series. One can easily distinguish a smooth, differentiable time series, for which $H \approx 1$ at small values of λ, from a nondifferentiable fractal curve, for which $0<H<1$. We have shown that the SF can be used in time series analysis also in the case when the time series is not affine, but there are in this case different scalings for different time scales. We have further shown that, in addition to the scaling properties, this method can also reveal (quasi)periodic features of the analysed data. The advantage of the method is that it conveniently visualises the periods of the analysed time series.

References

Akasofu, S.-I., Physics of magnetospheric substorms, D. Reidel Publishing Company, Dordrecht, Holland, 1977.

Baker, D.N., L.F. Bargatze, and R.D. Zwickl, Magnetospheric response to the IMF: Substorms, J. Geomag. Geoelectr., 38, 1047, 1986.

Baker, D.N., A.J. Klimas, R.L. McPherron, and J. Büchner, The evolution from weak to strong geomagnetic activity: An interpretation in terms of deterministic chaos, Geophys. Res. Lett., 17, 41, 1990.

Bargatze, L. F., D.N. Baker, R.L. McPherron, and E.W. Hones, Magnetospheric impulse response for many levels of geomagnetic activity, J. Geophys. Res., 90, 6387, 1985.

Brigham, E.O., The fast Fourier transform, Prentice-Hall Inc., Englewood Cliffs, N.J., 1974.

Burlaga, L.F., and L.W. Klein, Fractal structure of the interplanetary magnetic field, J. Geophys. Res., 91, 347, 1986.

Buzug, Th., and G. Pfister, Optimal delay time and embedding dimension for delay-time coordinates by analysis of the global static and local dynamical behavior of strange attractors, Phys. Rev. A Gen. Phys., 45, 7073, 1992.

Davis T.N., and M. Sugiura, Auroral electrojet activity index AE and its universal time variations, J. Geophys. Res.,71, 785, 1966.

Ding, M., C. Grebogi, E. Ott, T. Sauer, and J.A. Yorke, Plateau onset of correlation dimension: When does it occur?, Phys. Rev. Lett., 70, 3872, 1993a.

Ding, M., C. Grebogi, E. Ott, T. Sauer, and J.A. Yorke, Estimating correlation dimension from a chaotic time series; when does the plateau onset occur?, Physica D 69, 404, 1993b.

Eckmann, J.-P., and D. Ruelle, Ergodic theory of chaos and strange attractors, Rev. Mod. Phys., 57, 617, 1985.

Eckmann, J.-P., S. Oliffson Kamphorst, and D. Ruelle, Recurrence plots of dynamical systems, Europhys. Lett., 4, 973, 1987.

Egeland, A, Ø. Holter, and A. Omholt, Cosmical Geophysics, Universitetsforlaget, Oslo, Norway, 1973.

Feynman, J., and A. Ruzmaikin, Distributions of the interplanetary magnetic field revisited, Preprint, Jet Propulsion Laboratory, California Institute of Technology, Pasadena, California, 1993.

Fraser, A.M., and H.L. Swinney, Independent coordinates for strange attractors from mutual information, Phys. Rev. A Gen. Phys., 33, 1134, 1986.

Grassberger, P., and I. Procaccia, Measuring the strangeness of strange attractors, Physica 9D, 189, 1983.

Grassberger P., T. Schreiber, and C. Schaffrath, Nonlinear time sequence analysis, Int. J. Bif. and Chaos, 1, 521, 1991.

Greis N.P., and H.S. Greenside, Implication of a power-law power-spectrum for self-affinity, Phys. Rev. A, 44, 2324, 1991.

Hénon, M., A two-dimensional mapping with a strange attractor, Commun. Math. Phys., 50, 69, 1976.

Higuchi, T., Relationship between the fractal dimension and the power law index for a time series: a numerical investigation, Physica D 46, 254, 1990.

Hones, E.W., Transient phenomena in the magnetotail and their relation to substorms, Space Science Reviews, 23, 393, 1979.

Iyemori, T., H. Maeda, and T. Kamei, Impulse response of geomagnetic indices to interplanetary magnetic field, J. Geomagn. Geoelectr., 31, 1, 1979.

Kaplan, D.T., and L. Glass, Direct test for determinism in a time series, Phys. Rev. Lett., 68, 427, 1992.

Klimas A.J., D.N. Baker, D.A. Roberts, D.H. Fairfield, and J. Büchner, A nonlinear dynamical analogue model of geomagnetic activity, J. Geophys. Res., 97, 12253, 1992.

Koebbe, M., and G. Mayer-Kress, Use of recurrence plots in the analysis of time-series data, In M. Casdagli and S. Eubank, editors, Nonlinear modeling and forecasting, Vol. XII of SFI Studies In the Sciences of Complexity, Addison-Wesley, 1992.

Liebert, W., and H.G. Schuster, Proper choice of the time delays for the analysis of chaotic time series, Phys. Lett. A, 142, 107, 1989.

Lorenz, E.N., Deterministic nonperiodic flow, J. Atmos. Sci., 20, 130, 1963.

Mandelbrot, B., The Fractal Geometry of Nature, W.H. Freeman, New York, 1983.

Martien, P., S.C. Pope, P.L. Scott, and R.S. Shaw, The chaotic behavior of the leaky faucet, Phys. Lett. A, 110, 399, 1985.

Meyer-Kress, G., Application of dimension algorithms to experimental chaos, in Directions in Chaos, Vol. 1, ed. Hao Bai-Lin, World Scientific, Singapore, 1988.

Osborne, A. R., and A. Provenzale, Finite correlation dimension for stochastic systems with power-law spectra, Physica D 35, 357, 1989.

Osborne, A.R., and A. Pastorello, Simultaneous occurrence of low-dimensional chaos and colored random noise in nonlinear physical systems, Phys. Lett. A, 181, 159, 1993.

Packard, N.H., J.P. Crutchfield, J.D. Farmer, and R.S. Shaw, Geometry from a time series, Phys. Rev. Lett., 45, 712, 1980.

Panchev, S., Random functions and turbulence, Pergamon, Oxford, 1971.

Parks, G.K., Physics of space plasmas, Addison-Wesley Publishing Company, 350 Bridge Parkway, Redwood City, 1991.

Pavlos, G.P., G.A. Kyriakou, A.G. Rigas, P.I. Liatsis, P.C. Trochoutsos, and A.A. Tsonis, Evidence for strange attractor structures in space plasmas, Ann. Geophysicae, 10, 309, 1992.

Price, C.P., and D. Prichard, The non-linear response of the magnetosphere: 30 October 1978, Geophys. Res. Lett., 20, 771, 1993.

Prichard, D., and C.P. Price, Spurious dimension estimates from time series of geomagnetic indices, Geophys. Res. Lett., 19, 1623, 1992.

Prichard D., The correlation dimension of differenced AL data, Preprint, Department of Physics, University of Alaska, Fairbanks, 1993.

Prichard D., and C.P. Price, Is the AE index the result of nonlinear dynamics?, submitted to Geophys. Res. Lett., 1993a.

Prichard D., and C.P. Price, On the nonstationarity of the AE index, Preprint, Department of Physics, University of Alaska, Fairbanks, 1993b.

Priestley, M.B., Spectral analysis and time series, Academic Press, London, 1981.

Provenzale A., L. A. Smith, R. Vio, and G. Murante, Distinguishing between low-dimensional dynamics and randomness in measured time series, Physica D 58, 31, 1992.

Rapp P.E., A.M. Albano, T.I.Schmah, and L.A. Farwell, Filtered noise can mimic low-dimensional chaotic attractors, Phys. Rev. E, 47, 2289, 1993.

Roberts D.A., D.N. Baker, A.J. Klimas, and L.F. Bargatze, Indications of low dimensionality in magnetospheric physics, Geophys. Res. Lett., 18, 151, 1991.

Roberts, D. A., Is there a strange attractor in the magnetosphere?, J. Geophys. Res., 96, 16031, 1991.

Sauer T., J. A. Yorke, and M. Casdagli, Embedology, J. Stat. Phys., 65, 579, 1991.

Shan, L.-H., P. Hansen, C.K. Goertz, and R.A. Smith, Chaotic appearance of the AE index, Geophys. Res. Lett., 18, 147, 1991a.

Shan, L.-H., C.K. Goertz, and R.A. Smith, On the embedding-dimension analysis of AE and AL time series, Geophys. Res. Lett., 18, 1647, 1991b.

Sharma, A.S., D. Vassiliadis, and K. Papadopoulos, Reconstruction of low-dimensional magnetospheric dynamics by singular spectrum analysis, Geophys. Res. Lett., 20, 335, 1993a.

Sharma A.S., D. A. Roberts, D. Vassiliadis, A. J. Klimas, D. N. Baker, and K. Papadopoulos, Low dimensional attractor in magnetospheric dynamics, Preprint, GSFC, 1993b.

Shaw, R., The dripping faucet as a model chaotic system, The Science Frontier Express Series, Aerial Press, Santa Cruz, CA, 1984.

Sigeti, D., and W. Horsthemke, High-frequency power spectra for systems subject to noise, Phys. Rev. A, 35, 2276, 1987.

Sugihara, G., and R.M. May, Nonlinear forecasting as a way of distinguishing chaos from measurement error in time series, Nature, 344, 734, 1990.

Takalo, J., J. Timonen, and H. Koskinen, Correlation dimension and affinity of AE data and bicolored noise, Geophys. Res. Lett., 20, 1527, 1993.

Takalo, J. and J. Timonen, Characteristic time scale of auroral electrojet data, Geophys. Res. Lett., 21, Number 7, 1994.

Takalo, J., J. Timonen, and H. Koskinen, Properties of AE data and bicolored noise, J. Geophys. Res., in press, 1994a.

Takalo, J., J. Timonen, and H. Koskinen, Dynamics of the magnetosphere as determined from AE and AL data, In Chang T., editor, Physics of Space Plasmas, SPI Conference Proceedings and Reprint series, Number 13, Cambridge, MA, Scientific Publishers, in press, 1994b.

Takalo J., R. Lohikoski, and J. Timonen, Structure function as a tool in AE and Dst time series analysis, submitted to Geophys. Res. Lett., 1994c.

Takens, F., Detecting strange attractors in turbulence, in Dynamical systems and turbulence, Vol 898 of Lecture notes in Mathematics, 366, Springer-Verlag, New York, 1981.

Theiler, J., Spurious dimension from correlation algorithms applied to limited time series data, Phys. Rev. A, 34, 2427, 1986.

Theiler, J., Some comments on the correlation dimension of $1/f^{\alpha}$ noise, Phys. Lett. A, 155, 480, 1991.

Theiler, J., B. Galdrikian, A. Longtin, S. Eubank, and J.D. Farmer, Using surrogate data to detect nonlinearity in time series, In M. Casdagli and S. Eubank, editors, Nonlinear modeling and forecasting, Vol. XII of SFI Studies In the Sciences of Complexity, Addison-Wesley, 1992.

Tsurutani, B.T., M. Sugiura, T. Iyemori , B.E. Goldstein, W.D. Gonzalez, S.I. Akasofu, and E.J. Smith, The nonlinear response of AE to the IMF B_S driver: A spectral break at 5 hours, Geophys. Res. Lett., 17, 279, 1990.

Vassiliadis, D.V., A.S. Sharma, T.E. Eastman, and K. Papadopoulos, Low-dimensional chaos in magnetospheric activity from AE time series, Geophys. Res. Lett., 17, 1841, 1990.

Vassiliadis D., and I.A. Daglis, A diagnostic for input-output nonlinear system: the effect of a nonlinear filter on the correlation dimension, Preprint, Max-Planck-Institut für Aeronomie, 1993.

Voss, R. F., Random fractals: Self-affinity in noise, music, mountains, and clouds, Physica D 38, 362, 1989.

Vörös Z., Synergetic approach to substorm phenomenon, Magnetopheric substorms, Geophysical Monograph 64, American Geophysical Union, 1991.

Wayland, R., D. Bromley, D. Pickett, and A. Passamante, Recognizing determinism in a time series, Phys. Rev. Lett., 70, 580, 1993.

Wu, X., and Z.A. Schelly, The effect of surface tension and temperature on the nonlinear dynamics of the dripping faucet, Physica D 40, 433, 1989.

Zbilut, J.P., and C.L. Webber Jr., Embedding and delays as derived from quantification of recurrence plots, Phys. Lett. A, 171, 199, 1992.